# Lubricant Depletion and Disk-to-Head Transfer at the Head-Disk Interface in Hard Disk Drives

Rohit P. Ambekar and David B. Bogy,
Computer Mechanics Laboratory,
5146 Etcheverry Hall
Department of Mechanical Engineering
University of California
Berkeley, CA 94720

Email: rohit@cml.me.berkeley.edu

## Abstract

As the head-disk spacing reduces in order to achieve the areal density goal of 1Tb/in.$^2$, dynamic stability of the slider is compromised due to a variety of proximity interactions. Lubricant pickup by the slider from the disk is one of the major reasons for decrease in the stability as it contributes to meniscus forces and contamination. Disk-to-head lubricant transfer leads to lubricant pickup on the slider and also causes depletion of lubricant on the disk.

In this report we experimentally and numerically investigate the process of disk-to-head lubricant transfer using a half-delubed disk, and we propose a parametric model based on the experimental results. We also investigate the dependence of disk-to-head lubricant transfer on the disk lubricant thickness, lubricant type and the slider ABS design. It is concluded that disk-to-head lubricant transfer occurs without slider-disk contact and there can be more than one timescale associated with the transfer. Further, the transfer increases non-linearly with increasing disk lubricant thickness. Also, it is seen that the transfer depends on the type of lubricant used, and is less for Ztetraol than for Zdol. The slider ABS design also plays an important role, and a few suggestions are made to improve the ABS design for better lubricant performance.

## Introduction:

In a Hard Disk Drive (HDD), there exist multiple layers on the magnetic disk. On top of the magnetic layer there is a hard diamond-like carbon (DLC) overcoat of about 1-2nm to protect the magnetic layer against head crashes and corrosion. On top of the DLC, there exists a molecularly thin (~0.5-1.5nm) lubricant layer to reduce the friction and wear at the head-disk interface (HDI) and to further protect against corrosion.

In order to achieve the target areal recording density of 1 $Tb/in^2$ the head-disk physical spacing has to be reduced to about 2.5 nm. At such a small spacing a variety of proximity interactions such as intermolecular forces and electrostatic forces affect the ability of the slider to fly stably over the disk [1-2]. Lubricant pickup by the slider also substantially reduces the stability of the slider [3], and it also contributes to ABS contamination. During the lifetime operation of the drive this might become the most important factor affecting stability. The lubricant pickup is predominantly caused by disk-to-head lubricant transfer, which also causes lubricant depletion on the disk. Retention of lubricant on the disk as well as reduction of lubricant pickup on the slider are critical for HDI reliability, and hence it is important to study disk-to-head lubricant transfer and its dependence on various parameters.

In the lubricant layer on the disk part of the lubricant is bonded while the remaining is mobile. The bonded fraction helps in providing a permanent cover on the DLC to reduce friction and corrosion. It also resists critical failures during occasional slider-disk contact. The mobile fraction helps in replenishment of the lubricant at sites on the disk where lubricant depletion has occurred. The mobile fraction is also responsible for the disk-to-head lubricant transfer, which can be reduced by reducing the mobile fraction. However, it is known that

reliability of the HDI is greatly reduced by reduction in the mobile fraction, and it fails immediately in absence of any mobile lubricant. Hence, disk-to-head lubricant transfer is unavoidable, and it can be used favorably through proper design of the HDI, as it aids in quick replenishment of lubricant at the depleted sites.

Ma et. al. [4] showed that "negative" (sub-ambient) pressure sliders demonstrate disk-to-head lubricant transfer using a half-delubed disk approach. Marchon et. al. [5] proposed a model based on the Langmuir equation of evaporation-condensation incorporating the airbearing shear force, and they studied the dependence of disk-to-head lubricant transfer on lubricant thickness and molecular weight. Smallen et. al. [6] experimentally studied the dependence of disk-to-head lubricant transfer on the lubricant disjoining pressure. They used the area of lubricant pickup on the slider as a metric for the amount of disk-to-head lubricant transfer and concluded that the amount of lubricant pickup depends on the disjoining pressure and its slope. Since this method does not give the actual volume of transfer (some lubricant may also be sheared off behind the ABS, which is not accounted for) or an insight into the process of transfer, we used the half delubed disk method here to study disk-to-head lubricant transfer.

When a slider is flown on a half delubed disk, the disk-to-head lubricant transfer occurs in the lubed zone, while head-to-disk lubricant transfer happens in the delubed zone (Fig. 1). By calculating the volume of lubricant lost/gained by the lubed/delubed zones over time, the disk-to-head lubricant transfer can be studied. In this report we describe the experimental investigation of disk-to-head lubricant transfer and its dependence on three factors: lubricant thickness, lubricant type and ABS design. From the resulting quantitative data we arrive at a parametric model to describe the process of lubricant depletion and transfer and we compare

the experimental data to the existing model by Marchon et. al. [5]. The study aims to enhance our understanding of this phenomenon and help in designing a better interface with reduced lubricant pickup by the slider and better retention of lubricant on the disk.

## Experimental:

Three disks of different thicknesses of Zdol and Ztetrol were used in the experiments. Table 1 shows the total lubricant thickness for each type of disk along with the bonded and mobile fractions. These disks were half delubed using a delubing apparatus kept under a clean hood. The disks were lowered into a beaker of HFE-7100 until they were half immersed. They were kept immersed for 10 minutes and were then pulled out smoothly and left exposed to the atmosphere for 2 minutes for the HFE to evaporate. The time for which the disks were immersed was varied initially from 1 to 30 minutes. It was seen that the disk immersed for 5 minutes removed about 95% of the lubricant, if 100% was the amount of lubricant removed when the disk was immersed for 30 minutes. After the preparation of the half delubed disks, calibration of Candela OSA was done for Zdol and Ztetraol disks using half delubed disks of 3 different thicknesses with the results shown in Fig. 2. As HFE removes only the mobile fraction of lubricant the mobile lubricant thickness was considered to be the same as the lubricant step height.

Subsequently lubricant transfer experiments were conducted on the Candela OSA. Two different femto slider designs, shown in Fig. 3, were flown on a half delubed disk at constant linear velocity of 32.46 mps (10K@31mm) and the lubricant profiles were measured in-situ. Time histories of the lubricant profiles were obtained, which were further processed to obtain quantitative estimates of the amount of lubricant depleted from the lubed zone and the amount

transferred to the delubed zone. Fig. 4 outlines the steps in this post-processing, which was carried out in Matlab. After background subtraction and radial averaging in the lubed and the delubed zones (Fig. 4(a)), the resulting data was smoothed (Fig. 4(b) and (c)) and the area under the profile corresponding to depletion or transfer was calculated (Fig. 4(d)). Using a calibration constant of the lubricant and the radius of the track, the area calculated was converted into lubricant volume. Errors in volume calculations exist in this procedure due to the noisy data, radial averaging and post-processing. The errors due to the first two cannot be estimated, but they are systematic errors and hence should be similar for all data. The errors due to post-processing were determined by repeatedly calculating the lubricant volume from the lubricant profile for a few data points. The error ($6\sigma$) in post-processing was less than $500\mu m^3$ (10%) for data close to $5000\mu m^3$ and decreased to about $200\mu m^3$ (20%) for data close to $1000\mu m^3$. Thus the absolute value of the errors decreased, but the percentage value increased.

## Results and Discussion:

*A. Dynamics of Lubricant Transfer*

Experiments were conducted on Zdol disks with femto slider A (Fig. 3(a)) to study the dynamics of lubricant depletion and transfer. Figs. 5(a) and (b) show the time history of lubricant depletion and transfer for disks with 13.5Å thick lubricant (mobile fraction). It is seen that the rate of depletion as well as transfer is high initially and gradually reduces. It should be noted that there is a difference between the volumes of lubricant depleted and transferred. This is plotted in Fig. 5(c), and it was found to be most likely because the lubricant on the slider is sheared away by the airflow to deeper etches on the ABS behind the low flying areas and to the

edge of the slider behind the trailing pad. It is seen from Fig. 5(c) that the net lubricant depletion increases with time before reaching a steady-state for the thickness of 13.5Å. On re-running the experiment on a disk with 9.4Å thick lubricant without cleaning the slider used above, it was observed that there was very little net lubricant depletion (Fig. 5(c)). This is because the net lubricant depletion had already reached a steady-state in the previous experiment and more lubricant accumulation in the already filled areas of the slider could not be supported. This shows that the lubricant loss due to air shear is bounded and only occurs until the recessing areas behind the trailing pad are filled with lubricant. Hence, in operation, it can be assumed that there is no lubricant loss due to air shear and there exists a balance of lubricant transfer between the slider and the disk (unless lubricant pooling occurs on the slider due to ABS design, which is discussed later).

Fig. 6 shows the angular distribution of lubricant at various times. Fig. 6(a) displays the raw data as obtained from the OSA, which shows a background low frequency noise due to disk runout. Hence the raw data was conditioned by subtracting the data obtained at 0 minutes, which gave the net change in the lubricant profile at various time instants, and an idealized lubricant step profile was assumed for 0 minutes as shown in Fig. 6(b). From the profile at 1 minute (Fig. 6(b)), we see more depletion at the start of the lubed zone and more transfer at the start of the delubed zone. Shearing of lubricant from the lubed zone to the delubed zone cannot explain this as it would predict more depletion at the end of the lubed zone. Thus, the depletion and transfer observed are a result of disk-to-head lubricant transfer.

The observed angular distribution of the lubricant can be explained in the following way. Upon the start of the test there is not much lubricant on the slider. Hence, when the slider enters the lubed zone from the delubed zone it is in a ‘starved’ regime, while the disk is in a

'flooded' regime. Due to this there is a high rate of lubricant transfer from the disk to the slider. As the slider proceeds through the lubed zone there is more lubricant transfer so the slider approaches flooded regime. As the lubricant volume on the slider increases the rate of disk-to-head transfer decreases. Once the slider crosses from the lubed zone to the delubed zone, the slider now is in the flooded regime and the disk is in the starved regime. Thus, a similar process as described previously follows, and there is net lubricant transfer from the slider to the disk. Further, as the lubricant volume on the slider decreases so does the rate of transfer. This explains why there is more transfer at the beginning of the delubed zone at 1 minute in Fig. 6(b).

The above observations can be formulated into equations for disk-to-head lubricant transfer. If the lubricant volume on the slider and the disk is normalized by the area where the lubricant transfer occurs, the equations can be written in terms of lubricant thickness on the slider and the disk. Fig. 7 shows a schematic diagram of the lubricant transfer model. Let $h_1$, $h_2$ and $h_3$ be the disk lubricant thickness, slider lubricant thickness and the lubricant thickness of the sheared-off lubricant on the slider, respectively. If the disk track is discretized and the slider is over node i, then $h_1(i)$ is the disk lubricant thickness below the slider. The easiest relation that can be arrived at from the above observations is one in which the rate of transfer depends on the difference of lubricant thicknesses on the slider and the disk. Thus, we arrive at equation (1), which is the rate of lubricant transfer from the slider to the disk and $K_1$ is a constant of proportionality. The lubricant sheared off from the slider surface can be assumed to be a function of $h_2$ (proportional to $h_2^2$ if Couette flow is assumed). Hence $K_2$, the proportionality constant, is assumed to depend on $h_2$. From the experiments we see that as the accumulation ($h_3$) increases, the rate of accumulation goes down until it becomes zero at a

maximum allowable thickness $h_3^0$. This yields equation (2). Finally, equation (3) represents the mass balance at the HDI.

$$\frac{dh_1(i)}{dt} = K_1(h_2 - h_1(i)) \tag{1}$$

$$\frac{dh_2}{dt} = K_1(h_1(i) - h_2) - K_2(h_2)\cdot(h_3^0 - h_3) \tag{2}$$

$$\frac{dh_3}{dt} = -\frac{dh_1(i)}{dt} - \frac{dh_2}{dt} \tag{3}$$

Neglecting the shearing of the lubricant behind the ABS as it is only seen at the start and is negligible later, this is a linear system of equations and yields exponential solutions in time of the form $h\left(1-e^{-t/\tau}\right)$, where $\tau$ is a time constant. If we use such a solution to fit the lubricant depletion history in Fig. 5(a) we find that only one time constant cannot produce an effective fit, since the rate of depletion is very high at the start. Hence, at least two time scales must exist. A short time scale corresponds to the initial transfer after which a longer time scale sets in. Using two time scales we obtain an effective fit as shown in Fig.8 along with the fit equation.

The higher initial transfer rate is believed to be due to a total lack of mobile lubricant in the delubed zone. Thus the disjoining pressure is very high in the delubed zone which facilitates the high head-to-disk transfer rate (based on the evaporation-condensation model in [5] reproduced here in equation (5)). This also leads to a high disk-to-head transfer rate in the lubed zone as a source of replenishment of the slider lubricant. Once a small layer of mobile lubricant is formed in the delubed zone the disjoining pressure drastically reduces and so does the transfer rate. Fig. 6(b) shows the angular distribution of lubricant from 1 to 100 minutes. It

is seen that up until 3 minutes there is a large change in $h_1$ in the lubed and delubed zones. After 3 minutes, there is only a gradual change in $h_1$.

If there is a local depletion on the disk during operation of the drive the rate of lubricant replenishment due to the slider is thus expected to be a function of the difference between the average disk lubricant thickness and that in the depleted zone. The higher rate of transfer in the case of total depletion may be responsible for avoiding critical failures in case of total lubricant depletion in some region of the disk.

Equations (1-3) were simulated using different constants, and the results are shown in Fig. 9. Runge-Kutta methods of integration (from ODESuite in Matlab) took extremely long times for integration. Since the system of differential equations is linear ($K_2$=0), an implicit Euler method was then used for integration. Since this method is first order accurate as well as stable (hence convergent), reliable results are guaranteed for non-stiff problems, such as the current set of equations.

From the results in Fig. 9, it is seen that the simulated results qualitatively satisfy the experimental observations of the angular profile as well as the depletion history. A low value of $K_1$ produced a relatively flat angular profile which matched the experimental observations similar to the lubed zone in Fig. 6(b). A high value of $K_1$ produced steeper angular profiles, which matched better with the observations similar to the delubed zone (1 min) in Fig. 6(b). Lastly, it should be noted that the system of equations (1-3) is just a parametric system to understand the dynamics of disk-to-head lubricant transfer, and hence it is not able to explain the observed results quantitatively.

Using the information about the rate of lubricant transferred during the experiments, we can estimate the average lubricant volume on the trailing pad. We assume that the same

amount of lubricant is transferred during each rotation of the disk, and all of the lubricant collected on the slider in the lubed zone is transferred to the delubed zone in the first minute when there is no lubricant in the delubed zone. From Fig. 5(a) we see that the actual lubricant volume transferred in the first minute is 1654$\mu m^3$ for a disk lubricant thickness of 13Å. The slider passed over the delubed zone 10,000 times in 1 minute (=rpm). Thus, the total lubricant volume on the slider is estimated to be $1654\mu m^3/10^4$ =0.1654 $\mu m^3$. Further, the trailing pad area of the Femto A slider was determined to be $0.0122mm^2$ from image analysis. Thus, the average lubricant thickness on the trailing pad is 0.1654 $\mu m^3/0.0122mm^2$ = 0.013nm = 0.13Å. However, all of the trailing pad will not be covered by the lubricant, only the low flying areas close to the trailing edge will be covered.

*B. Dependence on Disk Lubricant Thickness*

Experiments were conducted on disks with three different lubricant thicknesses of Zdol. The ABS design A was used, shown in Fig. 2(a). The time histories of lubricant depletion, transfer and net depletion were recorded for 30 minutes for the various lubricant thicknesses and are shown in Figs. 10(a), (b) and (c).

From Figs. 10 (a) and (b) we see that the rate of depletion and transfer was high initially and decreased later, as explained in the previous section. The net lubricant depletion is plotted in Fig. 10(c). It is seen that the net depletion is very close to zero except in case of the 13Å thickness. Since this was the first test conducted there was no lubricant accumulation behind the ABS prior to the test. Hence, the net lubricant depletion became negligible for the subsequent tests after there was enough lubricant accumulation behind the ABS due to air shear, which occurred in the 13Å case.

Figs. 11 (a) and (b) show the lubricant depletion and transfer volumes after 30 mins for various disk lubricant thicknesses for two instances of same ABS design A along with the data fits. The relation between the disk lubricant thickness and the lubricant depletion/ transfer is observed to be monotonic and non-linear for Zdol. The monotonicity implies that there is more transfer and depletion for higher disk lubricant thickness. Thus, the slider lubricant thickness, which is responsible for the head-to-disk transfer, is higher for higher disk lubricant thickness. This can aid in meniscus formation and reduction of stability of the slider.

Data fits were performed on the experimentally obtained depletion and transfer volumes in Fig. 11 (a) and (b) to explore their non-linear dependence on the disk lubricant thickness. Since no depletion or transfer is expected for 0Å of mobile lubricant thickness, data was extrapolated to obtain better fits. For four points, a cubic polynomial produced an exact fit for the transfer data as seen in Fig. 11 (a), while only a quadratic polynomial was sufficient to fit the depletion data in Fig. 11(b).

The main reason for the non-linear relation between the disk lubricant thickness and the lubricant depletion/ transfer is the non-linear dependence of the lubricant disjoining pressure on the lubricant thickness. It is known that as the lubricant thickness increases the disjoining pressure reduces [6, 7]. Since the disjoining pressure is an indicator of the bonding strength of the lubricant to itself and the substrate, a lower value of disjoining pressure facilitates the lubricant transfer. This is in accordance with the condensation flux (the amount of lubricant condensed on the slider from the disk) as predicted by the lubricant transfer model based on evaporation-condensation [5].

According to this model in [5] the lubricant condensation flux $R_{cond}$ from disk-to-head is given by

$$R_{cond} = P_0 \sqrt{\frac{M_n}{2\pi RT}} \cdot \exp\left( - \frac{\pi(t_d) M_n}{\rho RT} \right) \quad (5)$$

where $P_0$ is the bulk vapor pressure, $M_n$ is the molecular weight, R is the gas constant, T is the absolute temperature, and ρ is the lubricant density. $\Pi(t_d)$ is the disjoining pressure for the disk lubricant thickness $t_d$. From $R_{cond}$, the volume flux of lubricant from disk-to-head can be calculated as $Q_{cond} = R_{cond}\, A/\rho$, where A is the cross-section area and ρ is the lubricant density.

Following the analysis in [5] and using the values given for various parameters therein, we plot the dependence of $Q_{cond}$ on $t_d$ in Fig. 13 for ZDol 4000. It indicates the non-linear dependence of the disk-to-head transfer (manifested as lubricant depletion in the experiments) on the disk lubricant thickness. Below 6Å, the transfer rate is extremely small because of a very high dispersive disjoining pressure ($\Pi^d$) (Fig. 13). The polar disjoining pressure ($\Pi^p$) is small in this range for Zdol 4000. Between 6 and 18Å, $\Pi^p$ is high and introduces almost a linearity in the transfer rate, which increases rapidly after 18Å due to low $\Pi^d$ and $\Pi^p$.

The evaporation flux (the amount of lubricant evaporated from the slider to the disk) is also given by equation (5) with $t_d$ replaced by $t_s$, the slider lubricant thickness. This indicates the same non-linear dependence of head-to-disk transfer (manifested as lubricant transfer in the experiments) on the slider lubricant thickness. We see from the experiments that the lubricant depletion and transfer volumes are the same, so we can conclude from this dependence that the slider and disk lubricant thicknesses are equal if the disjoining pressure curve for the lubricant as a function of lubricant thickness is the same for the slider and the disk. This would require the slider and disk DLC layers to be identical, which might not be the case as some efforts are being made to chemically modify the slider surface to decrease its surface energy [8]. In such a case, from equation (5) above, equality between evaporation and condensation fluxes implies an equality in $\Pi_d(t_d)$ and $\Pi_s(t_s)$, i.e. the lubricant thicknesses on the slider and the disk are such

that the disjoining pressures are equalized. Knowing the disjoining pressure curves for the slider and the disk we can determine $t_s$ as shown schematically in Fig. 14. If the surface energy of slider is lowered due to chemical modification or coating the disjoining pressure curve $\Pi_s(t)$ will be lower than $\Pi_d(t)$, implying that $t_s$ will be lower than $t_d$, as expected. This would mean less lubricant pickup by the slider, which leads to better stability [3].

Certain anomalies were also observed in the depletion and transfer data (Fig. 11(b)). In this figure we see that the lubricant transfer is more than the lubricant depletion in the 5Å Zdol case. Upon investigation it was discovered that the slider is capable of transferring the accumulated lubricant back to the disk at once, especially if the disk lubricant thickness is small. This is because the disjoining pressure is high for less lubricant on the disk and low for the accumulated lubricant on the slider causing large head-to-disk transfer. This causes lubricant pooling on the particular track, which may be as high as 20Å as observed in one case, and then it diffuses with a diffusion time constant of several minutes. The lubricant pool may lead to meniscus formation and reduced flyability, and it can also result in magnetic spacing loss. Thus, the ABS should be designed to avoid excessive lubricant accumulation.

*C. Dependence on Lubricant Type*

Experiments were conducted on disks with three different lubricant thicknesses of Ztetraol, and the results were compared to the Zdol results. The depletion and transfer volumes after 30mins are plotted in Figs. 15 (a) and (b) for both lubricants. It is seen that for the same disk lubricant thickness the depletion and transfer volumes for Ztetraol are less than those for Zdol after considering the error ($6\sigma$) in post-processing of the OSA data to be $200\mu m^2$ for a

calculated lubricant volume of about 1000μm$^2$. The anomalous data in Fig. 15(b) is a result of lubricant pooling, which was explained previously.

The difference in the observed rates of depletion and transfer for the two lubricants can be explained on the basis of the structures of Ztetraol and Zdol, as shown in Table 2. Ztetraol has four reactive -OH endgroups per chain as compared to Zdol, which has two. Because of this Ztetraol is known to bond stronger to the DLC than Zdol. This is also manifested in the higher viscosity [9] and lower mobility [9-10] of Ztetraol even at lower molecular weights. Due to this increased adherence of Ztetraol to the substrate it is more difficult for it to transfer to the slider. Also, once Ztetraol is transferred to the slider, it is more difficult to transfer it back to the delubed zone on the disk due to its strong adherence. This can explain the lower depletion and transfer rates for Ztetraol. In addition to the lubricant type, the type of carbon overcoat also determines the bond strength between the lubricant and carbon layer. Hence, it is estimated that the type of carbon overcoat ($CH_x$, $CN_x$, etc.) will have an effect on the rate of lubricant transfer. Deoras et. al. [11] reported that Zdol 2000 and 4000 have lower mobility on a $CN_x$ overcoat as compared to $CH_x$. Lower mobility, being an indicator of higher bond strength between lubricant and carbon, implies that disk-to-head lubricant transfer will be less for the $CN_x$ overcoat.

*D. Dependence on ABS Design*

ABS design is perhaps the most critical component in the HDI design. Different recommendations have been made to achieve small spacings, better load-unload characteristics, less fly height modulation, etc. However, the lubricant performance is also

extremely important to ensure reliability of the HDI. Therefore we investigated the dependence of disk-to-head lubricant transfer on the ABS design.

In this set of experiments two different ABS designs, as shown in Figs.2 (a) and (b), were used. A substantial difference in the amount of lubricant depletion was observed between the two sliders. Figs. 16 (a) and (b) plot the lubricant depletion and transfer for ZDol. A large difference between the depletion and transfer is seen in case of the Femto A. Such a pronounced difference between depletion and transfer is not observed for Femto B. When the ABS designs were observed under an optical microscope after the tests (Fig. 17 (a) and (b)), large lubricant accumulation was seen in the deep etched area behind the trailing pad in case of Femto A. Lubricant accumulation on the slider depletes lubricant on the disk and also causes loss in stability. Further, excessive lubricant accumulation can also lead to lubricant pooling on the disk. Thus, this is an undesirable characteristic of the ABS design, and it should be avoided.

The above observations can be explained on the basis of the mass flow lines from the static simulations of the ABS designs as shown in Figs.17 (c) and (d). In the case of Femto A it is seen that the mass is transported from over the sides of the trailing pad into the deep etches behind them. This results in a large lubricant accumulation since the deep etches have a large area and depth. In case of Femto B, only a small area with a low etch-step exists behind the trailing pad. Therefore, it is able to hold much less lubricant and thus does not allow excessive lubricant accumulation. Thus, deep etches behind low flying areas need to be avoided in order to avoid lubricant accumulation on the slider. Designs such as Femto A may be currently attractive as they have less area close to the trailing edge due to which there will also be less influence of intermolecular forces. However, this may also cause excessive lubricant

accumulation if the front of the trailing pad is designed as in Femto A. The reduction in area at proximity is achieved in Femto B by the introduction of a "sub-shallow etch step" [12] of 25 nm, the shape of which is such that excessive lubricant accumulation is avoided.

The above analysis only explains lubricant accumulation on the ABS, but it does not explain a more important observation, i.e. the large depletion in case of Femto A. Lubricant flow on the disk due to the slider depends on the airbearing pressure and shear stress and in the continuum formulation is given by equations (1-4) in [13]. This flow is expected to affect the disk-to-head lubricant transfer. A higher pressure or shear may result in greater depletion and transfer. Static simulations were conducted for both ABS designs at 10K rpm at 31mm with 0° skew. The pressure profiles for both of the designs from these simulations are shown in Figs. 18(a) and (b). The shear stress was also calculated based on the first order slip model according to equation (4) in [14], and it is plotted in Figs.18 (c) and (d). Further, the total shear experienced by a point on the disk is an integration of the shear stress along the length of the slider above that point, as the points on the slider along its entire length pass over that point on the disk. This calculated shear is plotted along the slider width in Figs. 18 (e) and (f) for Femto A and B, respectively.

From the pressure profiles of both ABS designs in Figs. 18(a) and (b), it is observed that design A has a slightly higher peak pressure. While this certainly can lead to more depletion, it cannot explain the large difference in depletion observed between the two designs. Further, the difference in the gradient of pressure is also negligible and cannot be the reason for more depletion in case of Femto A. Due to the higher pitch and roll of design A, it is seen from Figs. 18(e) and (f) that the shear in design A is actually less than design B. Thus, the pressure and shear profiles by themselves cannot explain the large difference in the depletion.

Further experimental investigation was carried out for both designs by monitoring the lubricant depletion and transfer after 5 minutes for each design at a particular fly height. The fly height of the sliders was varied by changing the rpm, which was reduced until the sliders went into contact with the disk. The AE sensor was set to a high gain to accurately monitor contact. The LDV was used to monitor the slider dynamics to determine if there was any change in the slider dynamics in the event of light contact not detected by AE.

When these experiments were conducted on the Zdol disks for each ABS design from a high rpm to low rpm, it was found that almost no lubricant depletion/transfer occurred at high rpm. The depletion/transfer rate did not increase significantly as the rpm was lowered until a point where there was a sudden increase in the depletion and transfer rates. This behavior was demonstrated by both ABS designs. There was no change in the root mean square (RMS) level of AE signal until at a much lower rpm where the slider went into contact (touchdown rpm). When the rpm is lowered beyond this point the depletion and transfer rates are expected to remained high and keep increasing with decreasing rpm due to the reduction in fly height as well as the pitch and roll.

Figs. 19 (a) and (b) show the lubricant depletion volume after 5 minutes for designs A and B, respectively, using a bar plot. The RMS AE signal is also plotted along with the depletion volume. From these figures is seen a “critical” rpm at which the rate of lubricant transfer is high and above which the rate is small. Further, the corresponding AE signal shows no change at the critical rpm, indicating no contact of the slider with the disk at that rpm. The FFT of the slider dynamics at various rpms is shown in Fig. 20, where it is seen that the frequency content of the slider dynamics did not change until there was slider-disk contact, which was also detected by AE. (The contact slider dynamics were not recorded for the Femto

A slider due to severe slider-disk contact.) Thus, AE and LDV measurements confirm that there is no physical slider-disk contact at the critical rpm leading to a higher transfer rate. (Even a light contact of the slider with the lubricant is detected by an AE sensor.) This implies that the observed disk-to-head lubricant transfer occurs without contact and therefore should be a result of condensation of the lubricant on the slider.

The touchdown rpm corresponds to the glide height of the disk, which was 3.5 nm on the disks used in the experiments. By means of static simulations (radius= 26 mm used for experiments), the change in the flying attitude was calculated as a function of rpm. From this we can calculate the minimum fly height of the sliders as a function of rpm. This is plotted in Fig. 21(a). The fly height corresponding to the critical rpm can be considered as the critical flying height for the lubricant transfer from disk to the slider. The difference between the critical flying height and the glide height is defined as the critical clearance.

It is seen that this critical clearance is higher for design A (6.95 -3.5 = 3.45 nm) than B (4.12-3.5 = 0.62 nm). Thus, slider B can fly lower without causing large lubricant depletion and therefore has a better reliability. The existence of a critical clearance also explains the large difference in the depletion occurring with designs A and B as the lubricant depletion and transfer volumes plotted in Fig. 16 correspond to an rpm of 12.1K @26 mm (=10K@31mm). This rpm is clearly above the critical rpm of design B, but it is lower than the critical rpm of design A. Thus we observe high depletion for design A and low depletion for design B.

Figs. 22 (a) and (b) show the OSA scans of depletion and transfer above and below the critical rpm respectively for design A. Similar scans are shown in Figs.22 (c) and (d) for design B. The golden color corresponds to lubricant depletion while the black color corresponds to

lubricant accumulation. A large amount of depletion and transfer is seen below the critical rpm for both of the designs on the track corresponding to the location of the trailing pad.

From the experiments we conclude that the rate of condensation of the lubricant from the lubed part of the disk to the slider as well as the rate of evaporation of lubricant from the slider to the delubed part of the disk are dependent on the head-disk clearance. The rates are expected to increase as the clearance decreases. This has not been included in the evaporation-condensation model in [5], and it is a direction for future work.

## Conclusions

In this report we experimentally and numerically investigated the process of disk-to-head lubricant transfer using a half-delubed disk and a parametric model based on the experimental results. We also compared some of the experimental results with a physical model based on evaporation-condensation. Further, the dependence on disk-to-head lubricant transfer on the disk lubricant thickness, lubricant type and the slider ABS design was investigated. From the study we conclude the following:

(a) Substantial disk-to-head lubricant transfer can occur without slider-disk contact and more than one timescale can be associated with the transfer. While disk-to-head lubricant transfer aids in lubricant replenishment in areas where lubricant depletion occurs, it also leads to lubricant pickup by the slider leading to meniscus forces and contamination at the HDI causing reduced stability.

(b) The disk-to-head lubricant transfer increases non-linearly with increasing disk lubricant thickness, and this can be explained on the basis of disjoining pressure of the lubricant.

(c) The disk-to-head lubricant transfer depends on the type of lubricant used and is less for Ztetraol than for Zdol. This is because Ztetraol adheres more strongly to the substrate than Zdol.

(d) The disk-to-head lubricant transfer also depends on the ABS design. A critical clearance exists for each ABS design at which the transfer rate is high and above which the transfer rate is small. For better lubricant performance the ABS should be designed such that this critical clearance is as small as possible, i.e. the critical rpm is as close to the touchdown rpm as possible.

(e) Certain ABS features can lead to excessive lubricant accumulation on the slider. This in turn leads to lubricant pooling on the disk as the slider is capable of transferring some of the accumulated lubricant back to the disk. Lubricant pooling on the disk is undesirable as it can lead to magnetic spacing loss as well as a reduction in stability. Thus, these ABS features should be avoided.

## Acknowledgements:

The authors would like to thank Dr. Singh Bhatia and Dr. Robert Waltman of Hitachi GST for helpful discussions and for providing the disks used for this study. Thanks are also due to Takeshi Watanabe of Fuji Electric for providing some of the disks. RPA would also like to thank Leonard Gonzaga of DSI Singapore for providing some simulation data.

This work was supported by the Computer Mechanics Laboratory at the University of California, Berkeley, USA and the Information Storage Industry Consortium's EHDR Program.

## References:


[1] R.P. Ambekar, V.Gupta and D.B. Bogy, "Experimental and numerical investigation of the dynamic instability in the head-disk interface at proximity," *ASME J. Tribol.*, vol. 127, no. 3, pp. 530-36, July 2005.

[2] V. Gupta and D.B. Bogy, "Dynamics of sub-5-nm air-bearing sliders in the presence of electrostatic and intermolecular forces at the head-disk interface," *IEEE Trans. Magn.*, vol. 41, no. 2, pp. 610-15, Feb 2005.

[3] R.P. Ambekar and D.B. Bogy, "Effect of Slider Lubricant Pickup on Stability at the Head-Disk Interface," *IEEE Trans. Magn.*, vol.41, no.10, pp. 3028-30, Oct. 2005.

[4] X. Ma, H. Tang, M. Stirniman and J. Gui, "Effect of Slider on Lubricant Loss and Redistribution," *IEEE Trans. Magn,* Vol. 38, Vol. 5, 2144-46, Sept. 2002.

[5] B. Marchon, T. Karis, Q..Dai and R. Pit, "A model for lubricant flow from disk to slider," *IEEE Trans. Magn.*, vol. 39, no. 5, pp.2447-2449, Sept. 2003.

[6] M. J. Smallen and H. W. Huang, "Effect of disjoining pressure on disk-to-head lubricant transfer," *IEEE Trans. Magn.*, vol. 39, no. 5, pp.2495-2497, Sept. 2003.

[7] R.J. Waltman, A. Khurshudov and G.W. Tyndall, "Autophobic Dewetting of Perfluoropolyether Films on Amorphous Nitrogenated Carbon Surfaces," *Trib. Lett.*, Vol. 12, No. 3, pp. 163-69, Apr. 2002.

[8] H. Chiba, T. Musashi , Y. Kasamatsu, J. Watanabe, T. Watanabe, K. Watanabe, "Chemically modified air-bearing surface for the near-contact regime," *IEEE Trans. Magn.*, vol.41, no.10, pp. 3049-51, Oct. 2005.

[9] B.G. Min, J.W. Choi, H.R. Brown, D.Y. Yoon, T.M. O'Connor and M.S. Jhon, "Spreading characteristics of thin liquid films of perfluoropolyalkylethers on solid

surfaces. Effects of chain-end functionality and humidity," *Trib. Lett.*, Vol. 1, No. 3, pp. 225-32, Nov. 1995.

[10] T.E. Karis, W.T. Kim and M.S. Jhon, "Spreading and Dewetting in Nanoscale Lubrication," *Trib. Lett.*, Vol. 18, No. 1, pp. 27-41, Jan. 2005.

[11] S.K. Deoras, S-W. Chun, G. Vurens and F.E. Talke, "Spreading and Mobility Analysis of PFPE Lubricants using Surface Reflectance Analyzer (SRA)," *Tribol. Int.*, Vol. 36, No. 4-6, pp. 241-46, Apr.-Jun. 2002.

[12] L. Gonzaga and B. Liu, "Fabrication and Evaluation of Panda II design," INSIC Research Presentation.

[13] R.P. Ambekar and D.B. Bogy, "Slider-Lubricant Interactions at the Head-Disk Interface," CML Report 2006-07, May 2006 (Presented at MIPE 2006, Santa Clara, CA).

[14] D. Chen and D.B. Bogy, "A Comparison of Two Rarefaction Models in the Compressible Reynolds Equation Used in Air Bearing Design for Hard Disk Drives," CML Report 2005-10, Sept. 2005.

## Tables

| | Bonded (Å) | Mobile (Å) | Total (Å) |
|---|---|---|---|
| Zdol | 2.9 | 5.0 | 7.9 |
| | 2.9 | 9.4 | 12.3 |
| | 3 | 13.5 | 16.5 |
| Ztetraol | 5.8 | 2.2 | 7.9 |
| | 5.9 | 5.1 | 11.0 |
| | 8.1 | 5.9 | 14.0 |

**Table 1: Lubricant thicknesses of various disks used for experiments**

| | |
|---|---|
| Zdol | $HO\text{-}CH_2CF_2[(OCF_2CF_2)_p(OCF2)_q]OCF_2CH_2\text{-}OH$ |
| Ztetraol | $HO\text{-}CH_2\underset{\displaystyle OH}{\underset{\vert}{C}}HCH_2OCH_2CF_2[(OCF_2CF_2)_p(OCF2)_q]OCF_2CH_2\underset{\displaystyle OH}{\underset{\vert}{C}}HCH_2\text{-}OH$ |

**Table 2: Chemical structures of Zdol and Ztetraol**

## Figures:

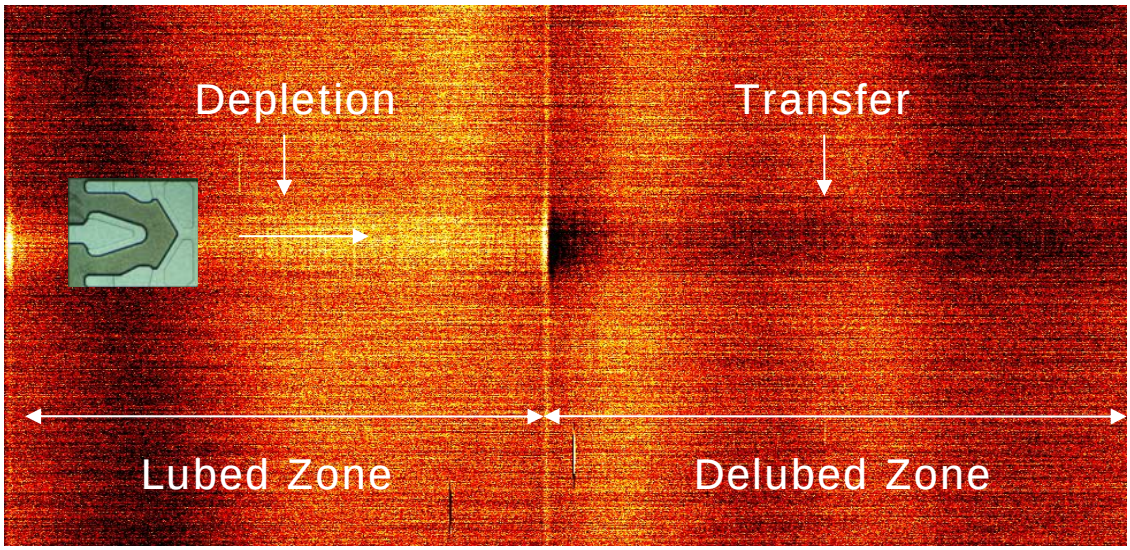


**Figure 1: OSA trace showing depletion and transfer in lubed and delubed zones respectively**

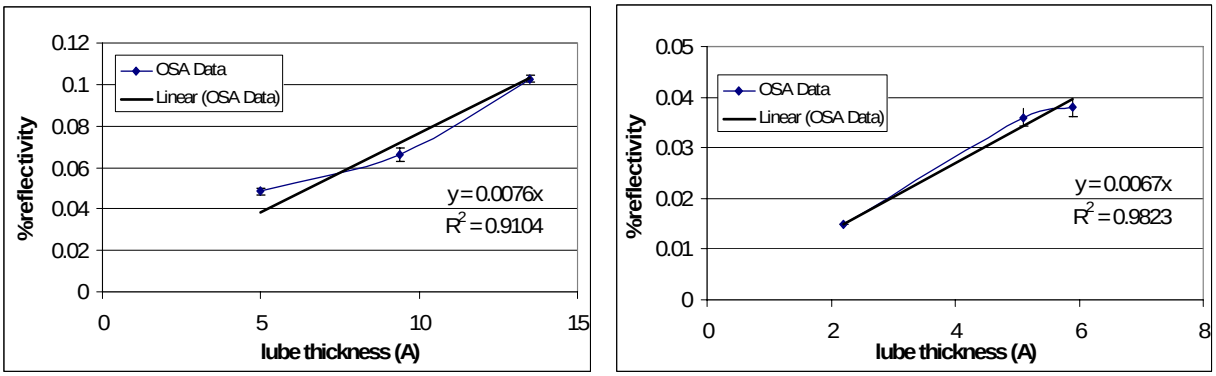


(a) (b)

**Figure 2: OSA Calibration: (a) Zdol and (b) Ztetrol**

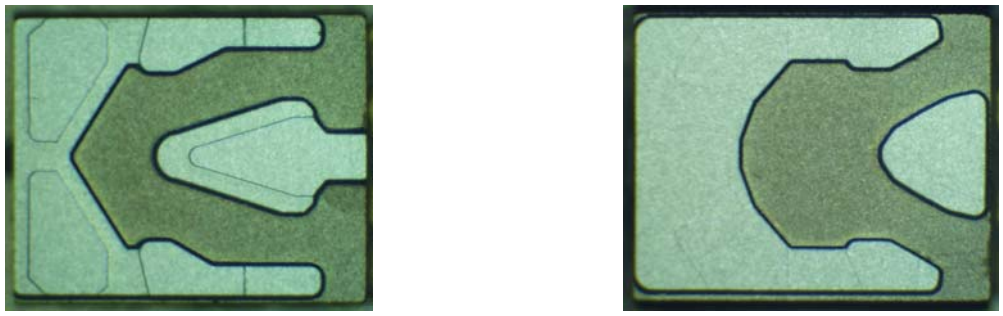

(a) (b)

**Figure 3: ABS designs used for experiments: (a) Femto A; (b) Femto B**

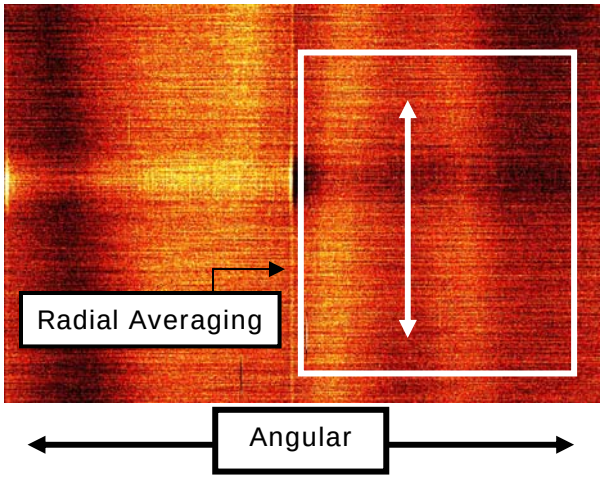


(a)

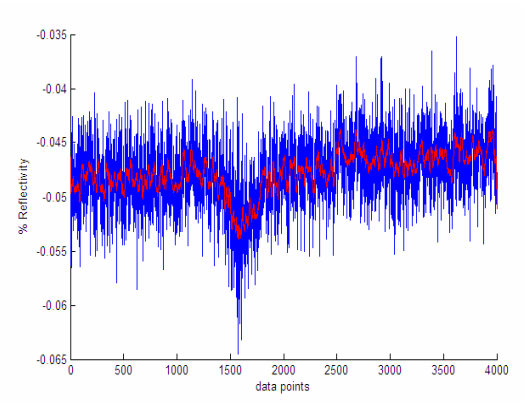


(b)

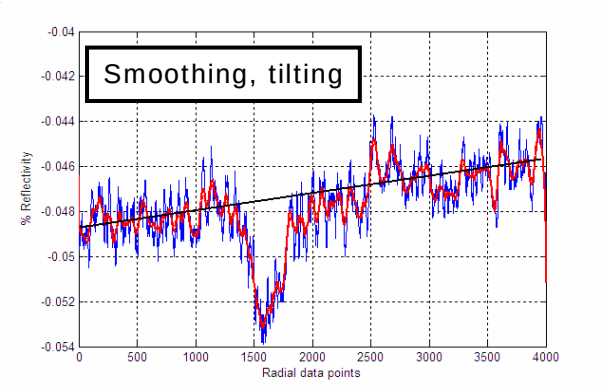


(c)

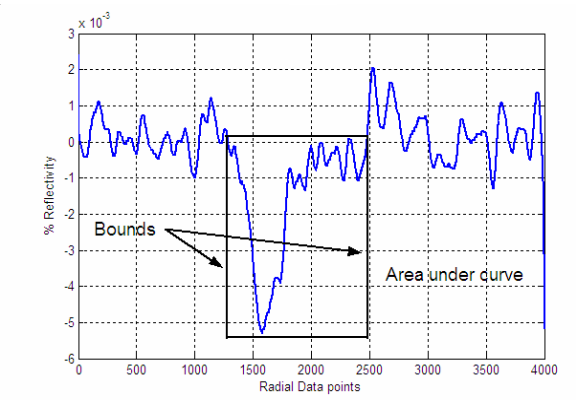


(d)

**Figure 4: Successive operations on the OSA trace to obtain lubricant transfer volume: (a) Radial averaging to OSA trace; (b) Filtering the data (blue) obtained from (a) to get smooth data (red); (c) Further smoothing and changing the background reflectivity to zero by tilting; (d) Integrating area under the reflectivity curve**

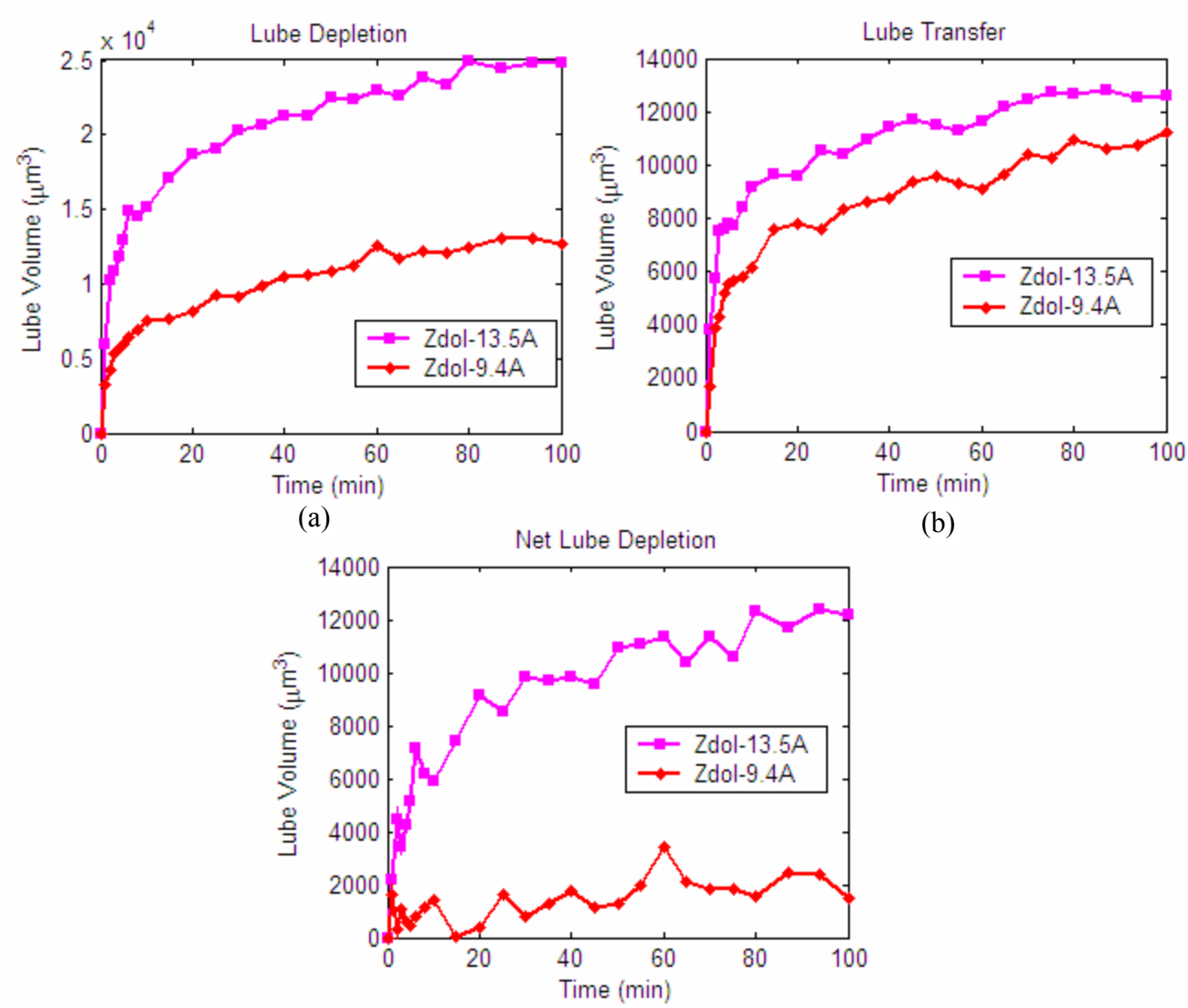


**Figure 5: Time history of (a) Lubricant depletion volume; (b) Lubricant transfer volume; (c) Net depletion volume for Femto A with Zdol lubricant**

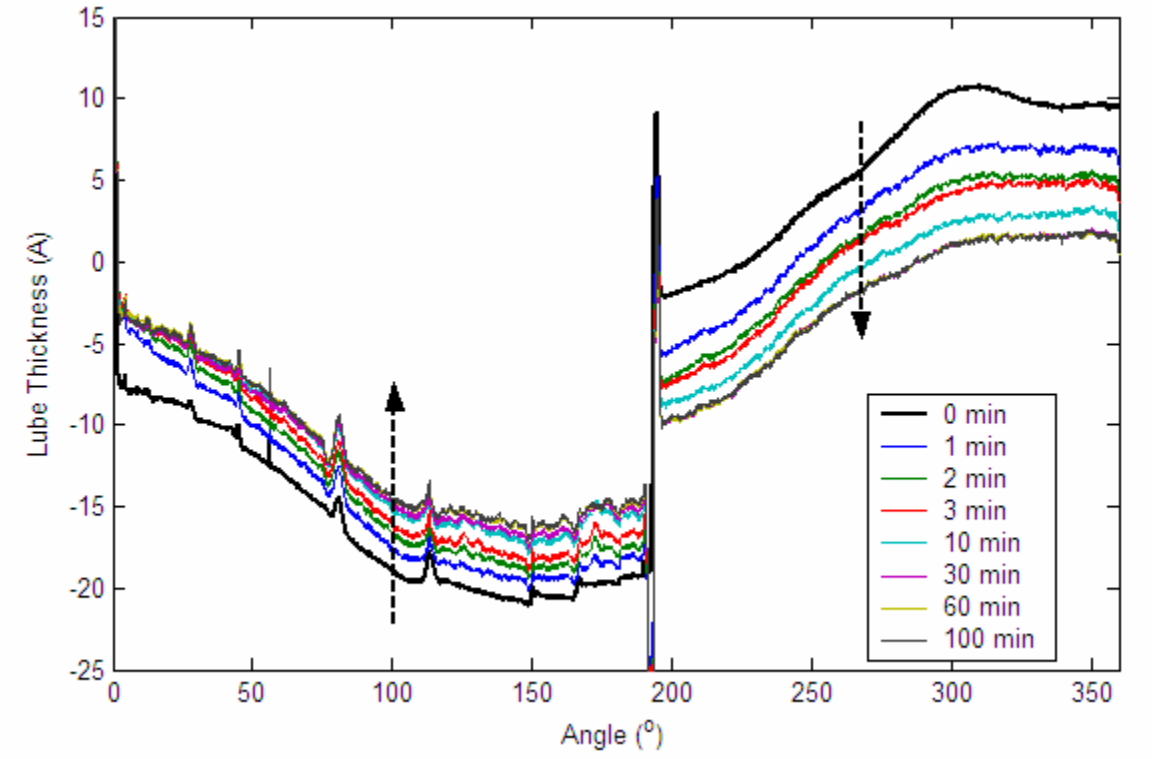


(a)

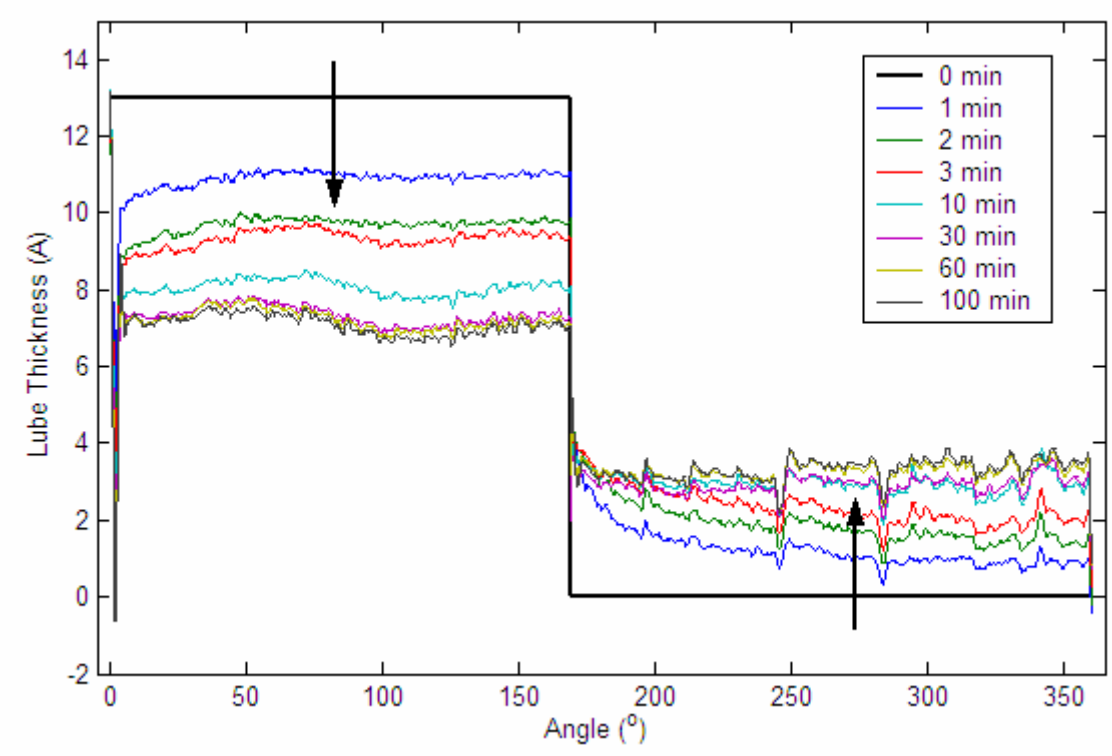


(b)

**Figure 6: Angular distribution of the lubricant (a) Original data from OSA; (b) Conditioned data of (a)**

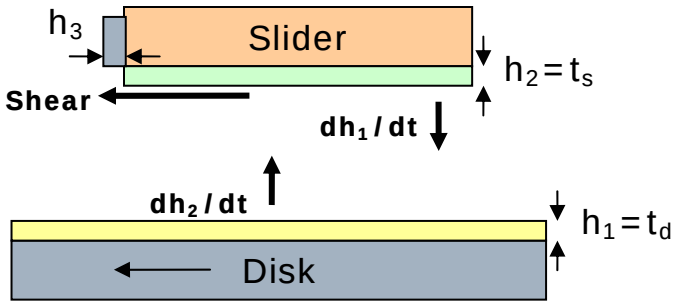


**Figure 7: Schematic of lubricant flow between the slider and the disk**

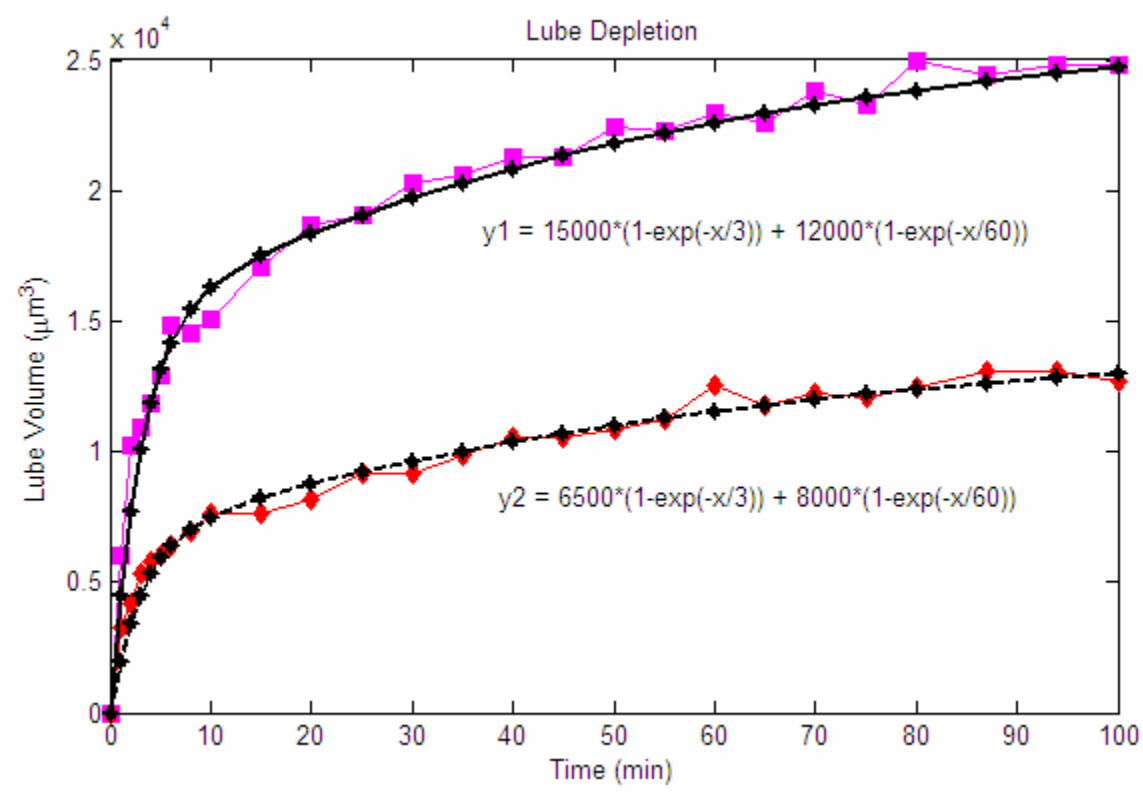


**Figure 8: Data fit to lubricant depletion volume showing two time scales**

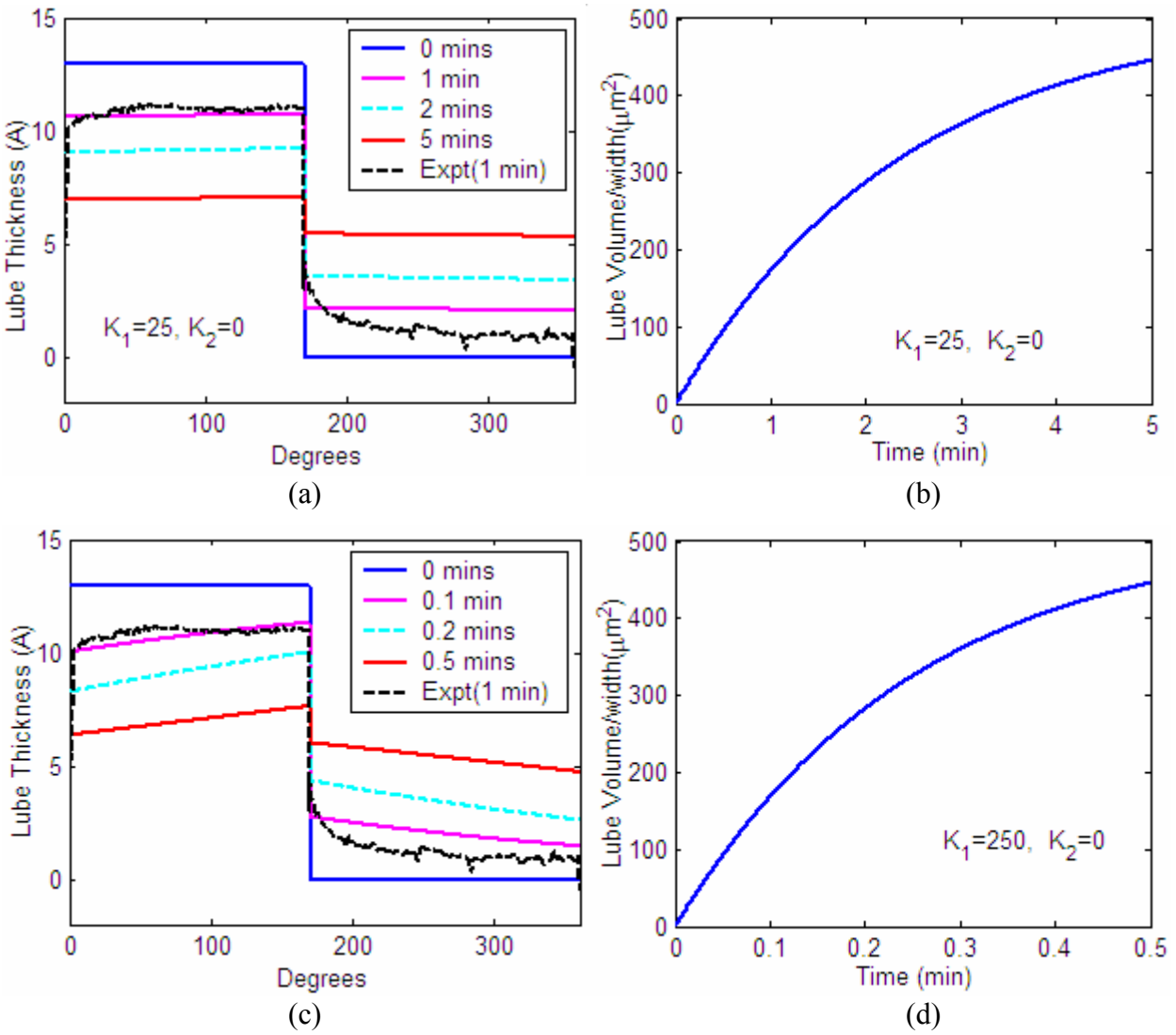


**Figure 9: (a),(b) Angular distribution and transfer history for low value of $K_1$, respectively; (c),(d) Angular distribution and transfer history for high value of $K_1$, respectively**

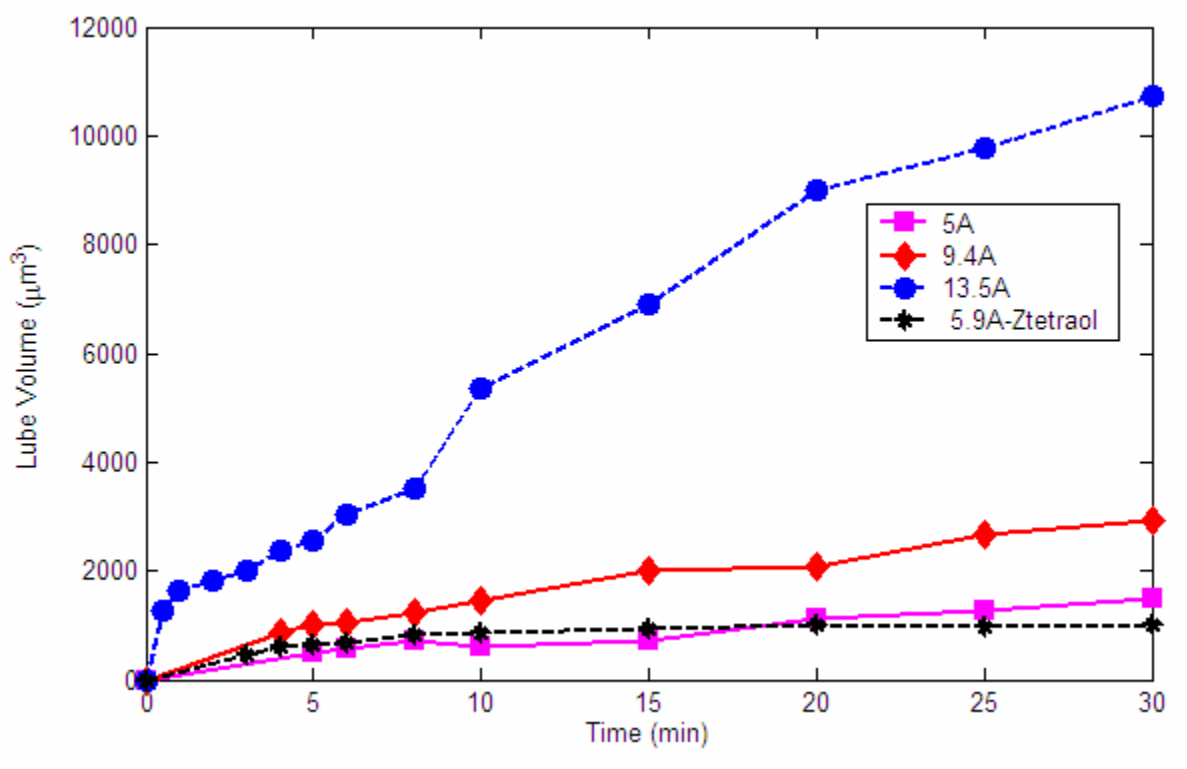
Lube Volume (μm3)
Time (min)
5A
9.4A
13.5A
5.9A-Ztetraol

(a)

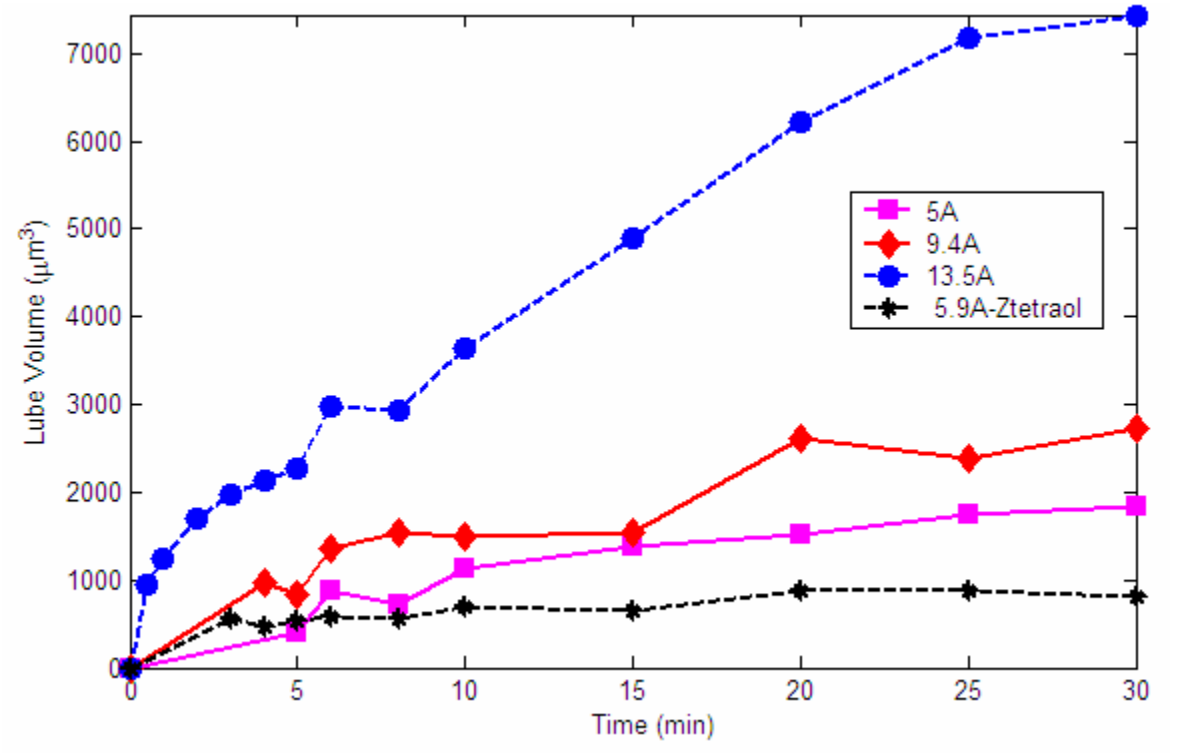
Lube Volume (μm3)
Time (min)
5A
9.4A
13.5A
5.9A-Ztetraol

(b)

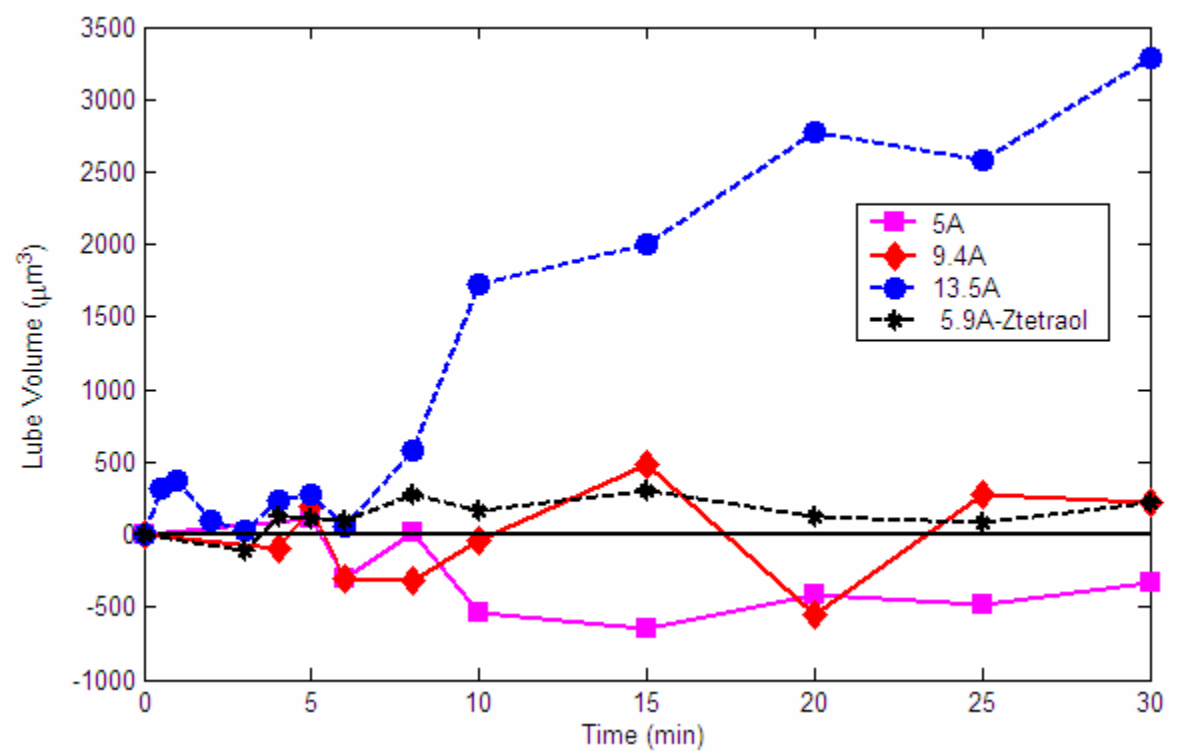


(c)

**Figure 10: Lubricant depletion and transfer for different thicknesses of Zdol:**
**(a) Lubricant depletion in the lubed zone; (b) Lubricant transfer to the delubed zone; (c) Net lubricant depletion**

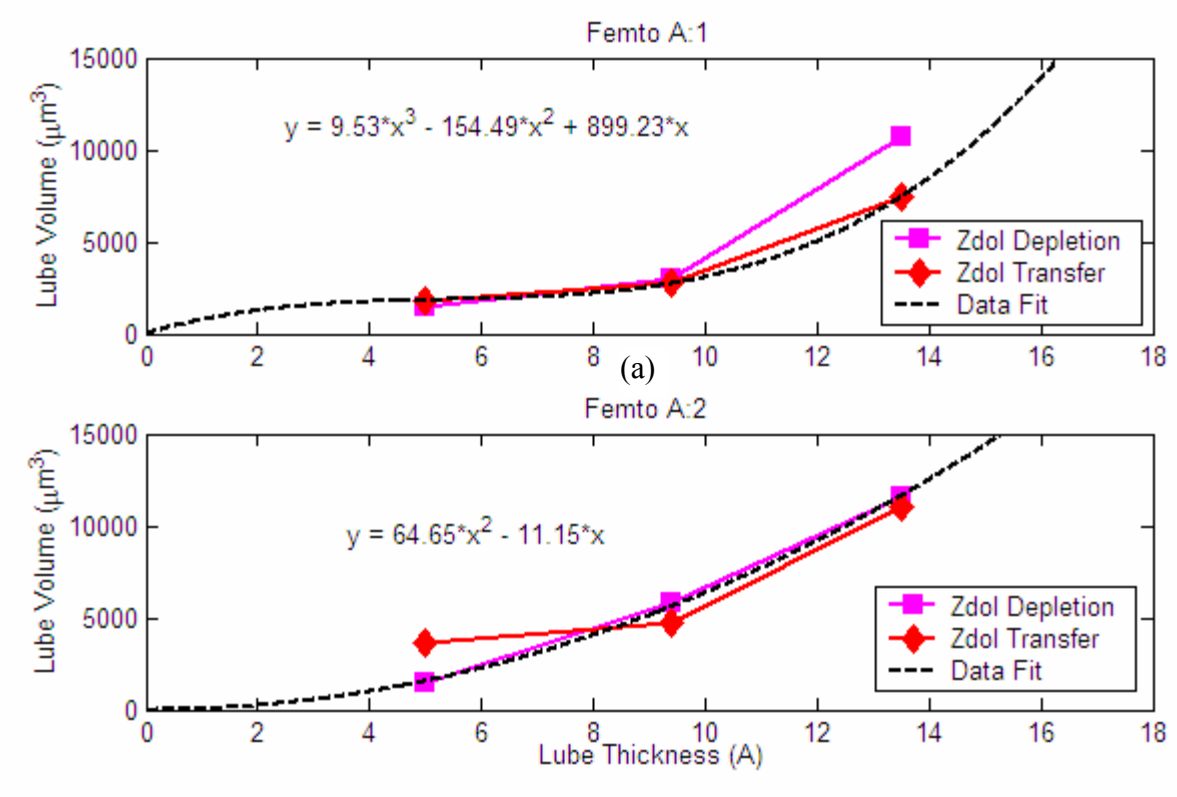


**Figure 11: Total lubricant depletion and transfer after 30 minutes along with data fits**

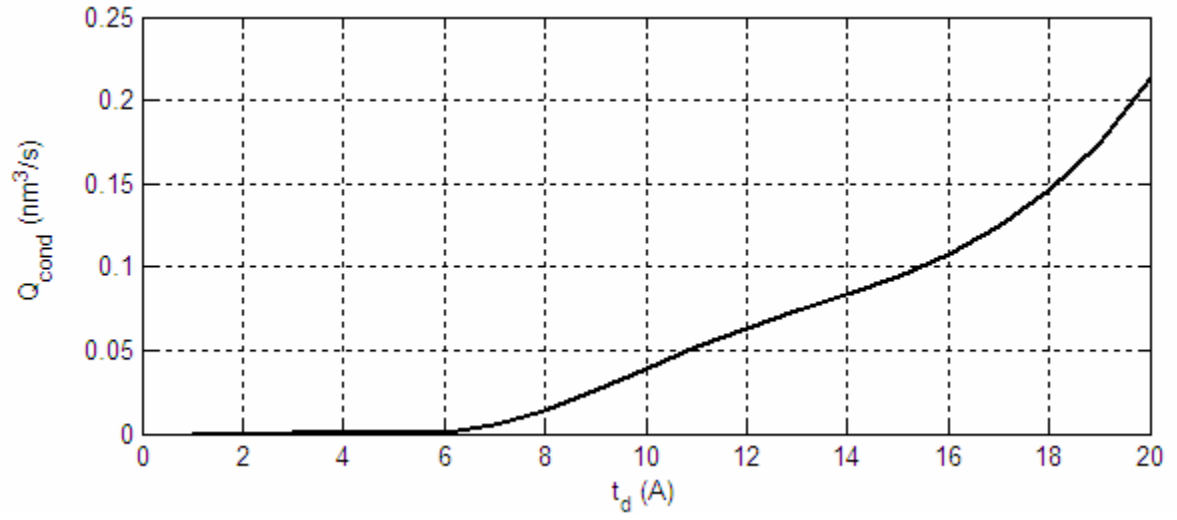


**Figure 12: Volume rate of lube transfer as a function of disk lubricant thickness as predicted by evaporation model of [5]**

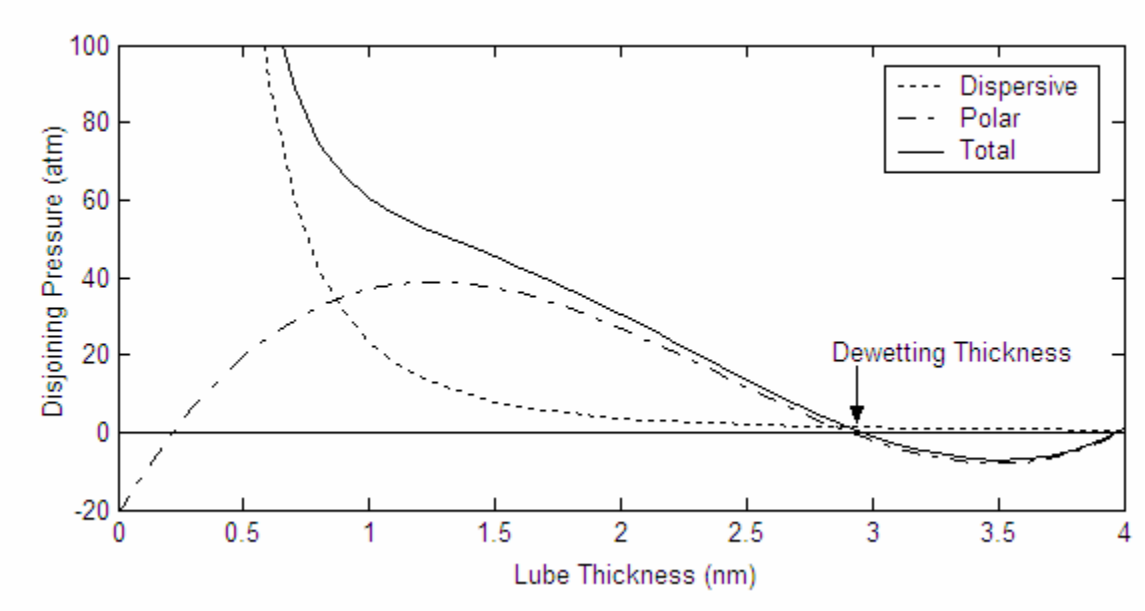


**Figure 13: Dependence of disjoining pressure lubricant thickness for Zdol 4000 [7].**

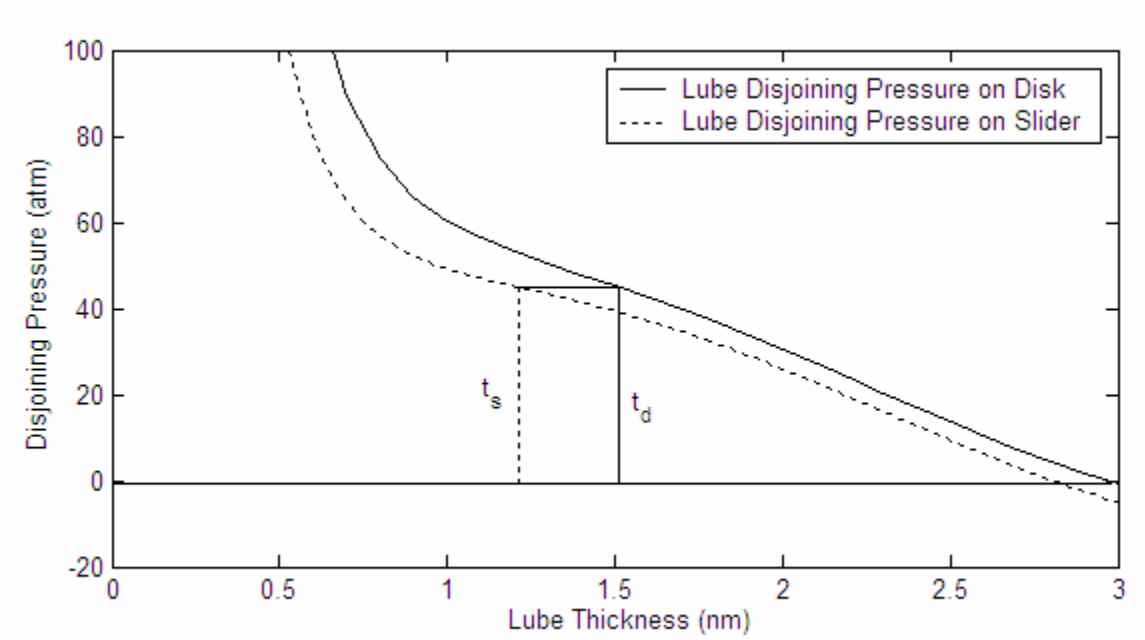


**Figure 14: Determining the slider lubricant thickness ($t_s$) knowing the disjoining pressure curves and the disk lubricant thickness ($t_d$)**

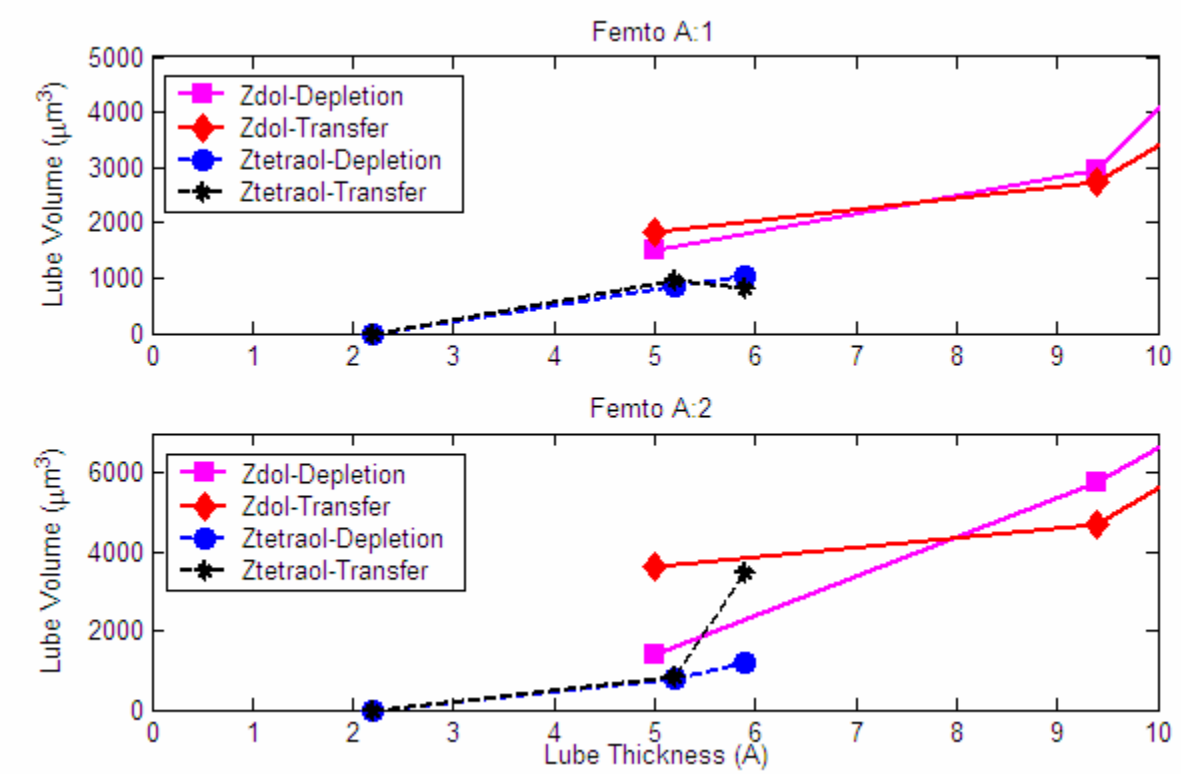


**Figure 15: Effect of lubricant type on the lubricant depletion and transfer**

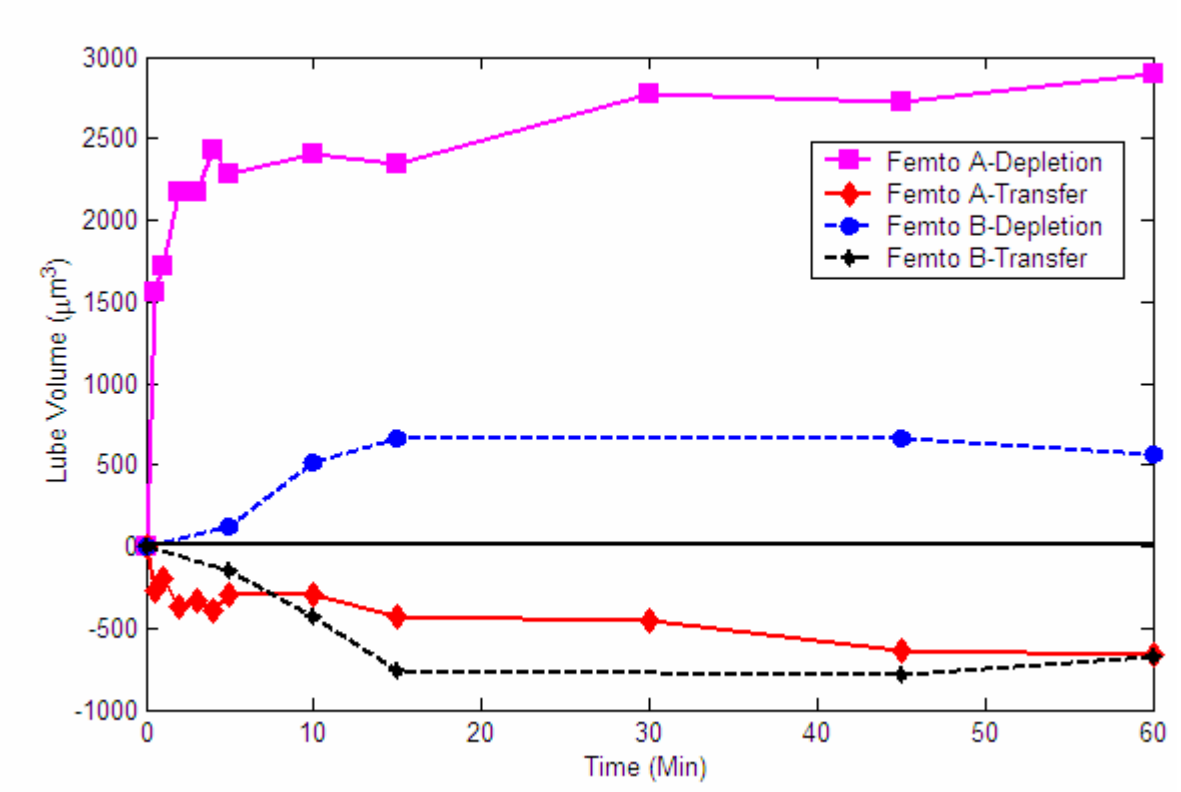


**Figure 16: Effect of ABS design on the lubricant depletion and transfer**

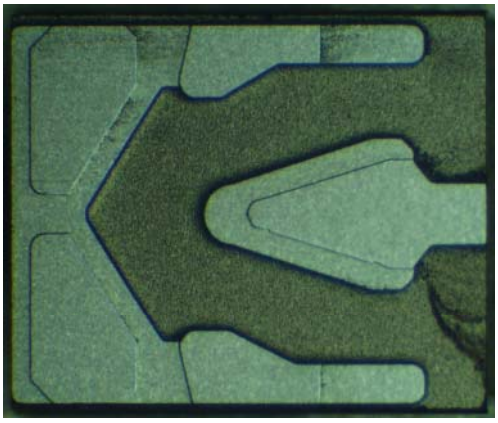

(a)

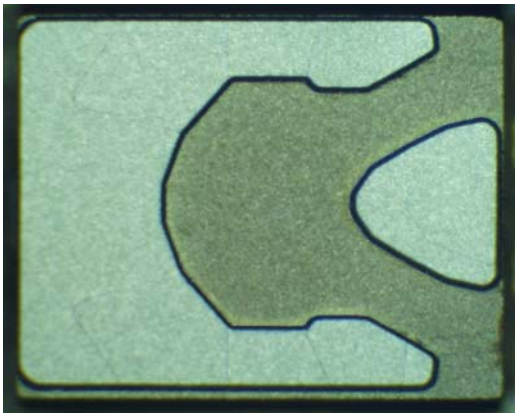

(b)

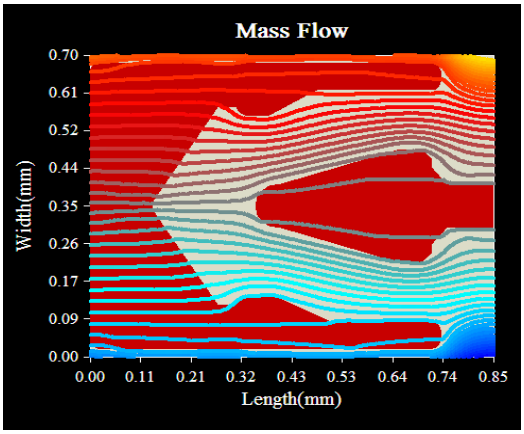


(c)

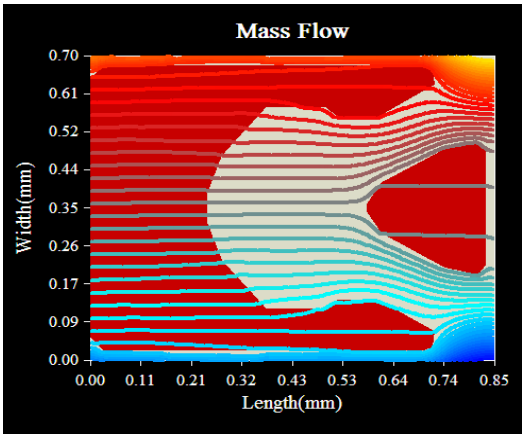


(d)

**Figure 17: (a), (b): ABS of Femto A and B, respectively, as seen under optical microscope after experiments; (c), (d): Mass flow lines across ABS for Femto A and B, respectively, as obtained from static simulations in CMLAir.**

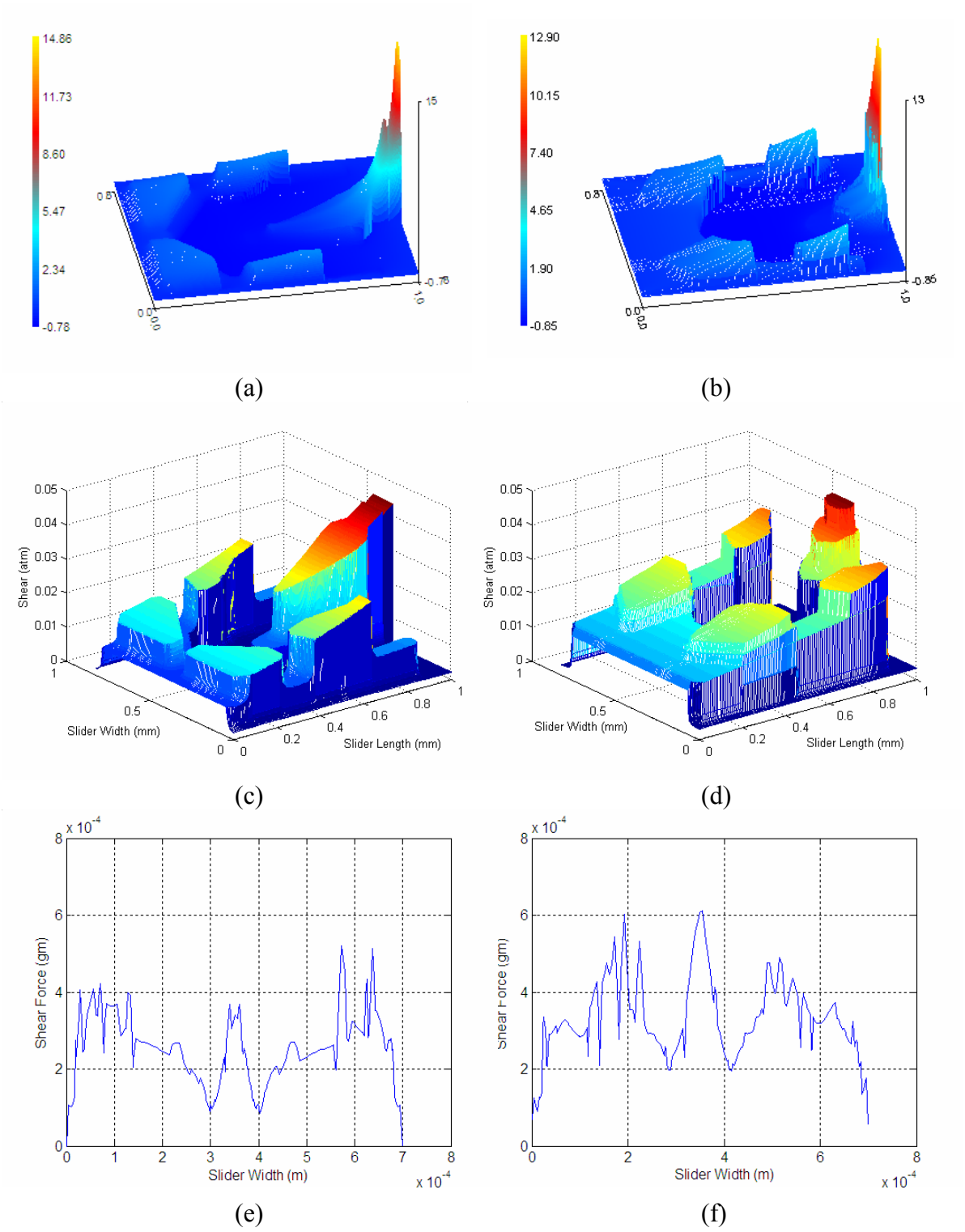


**Figure 18: (a),(c),(e) Pressure distribution, shear stress and shear/unit width for Femto A, respectively; (b),(d),(f) Pressure distribution, shear stress and shear/unit width for Femto B, respectively**

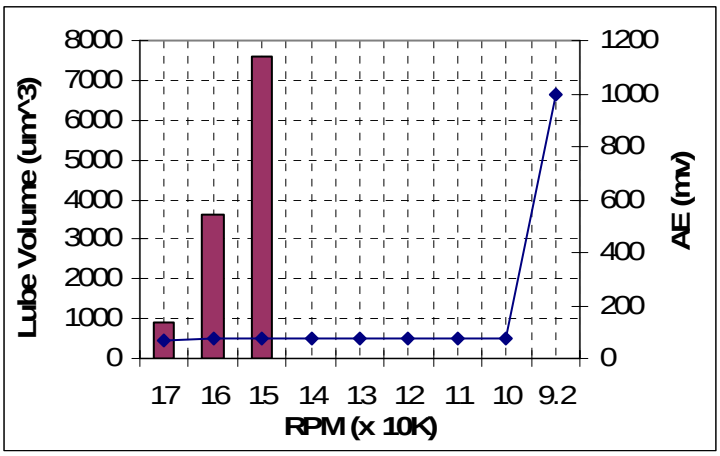


(a)

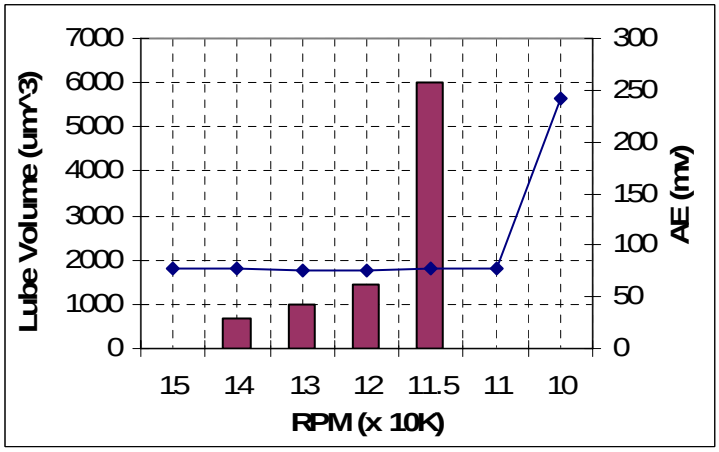


(b)

**Figure 19: Lubricant depletion volume and RMS AE signal at different rpms : (a) Femto A ; (b) Femto B**

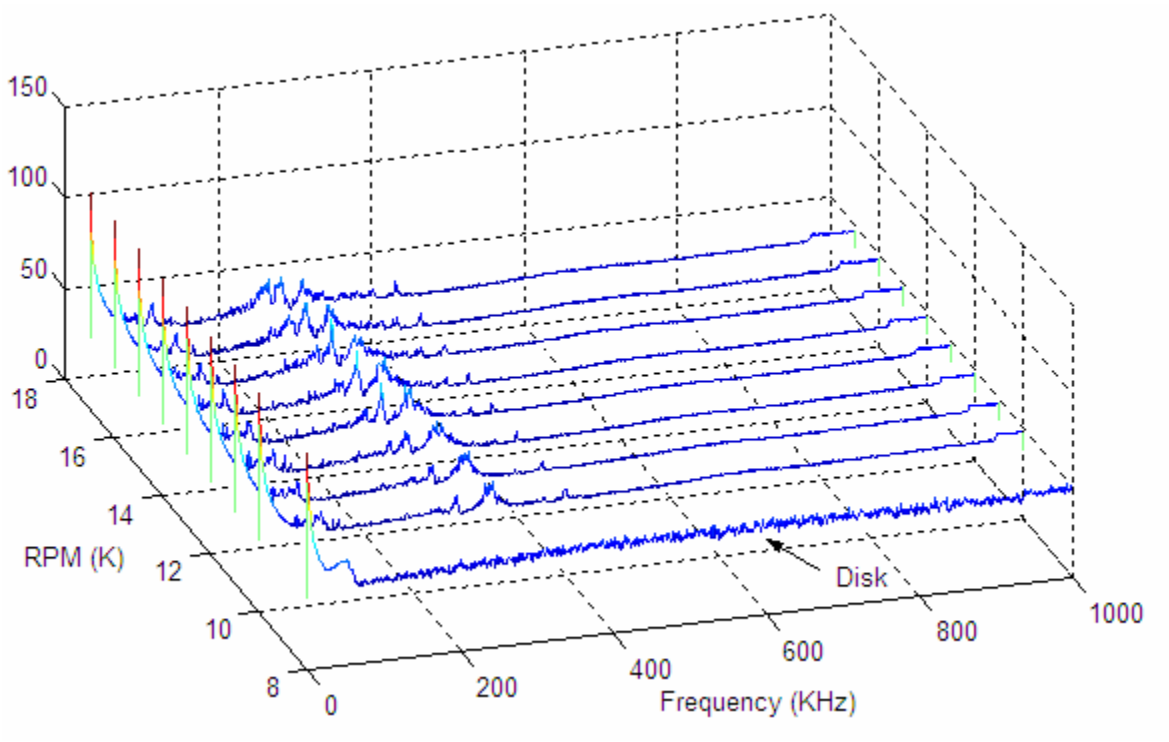


(a)

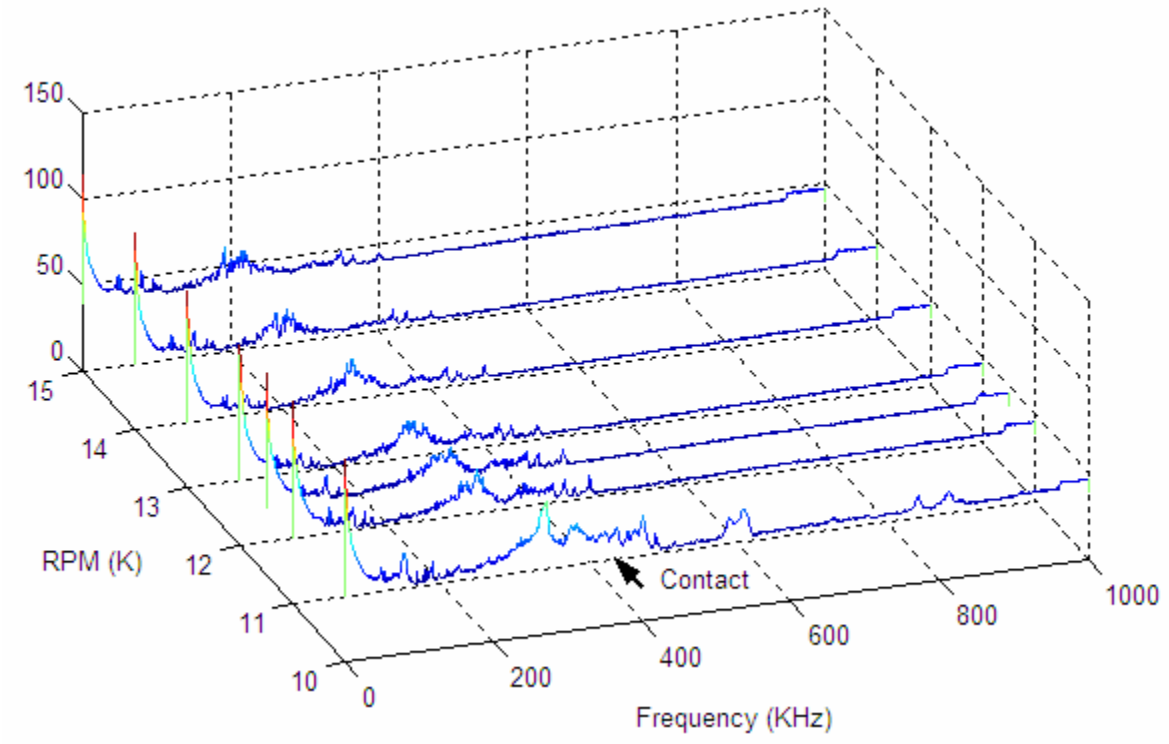


(b)

**Figure 20: Frequency content of slider dynamics as measured by LDV at different rpms for (a) Femto A and (b) Femto B**

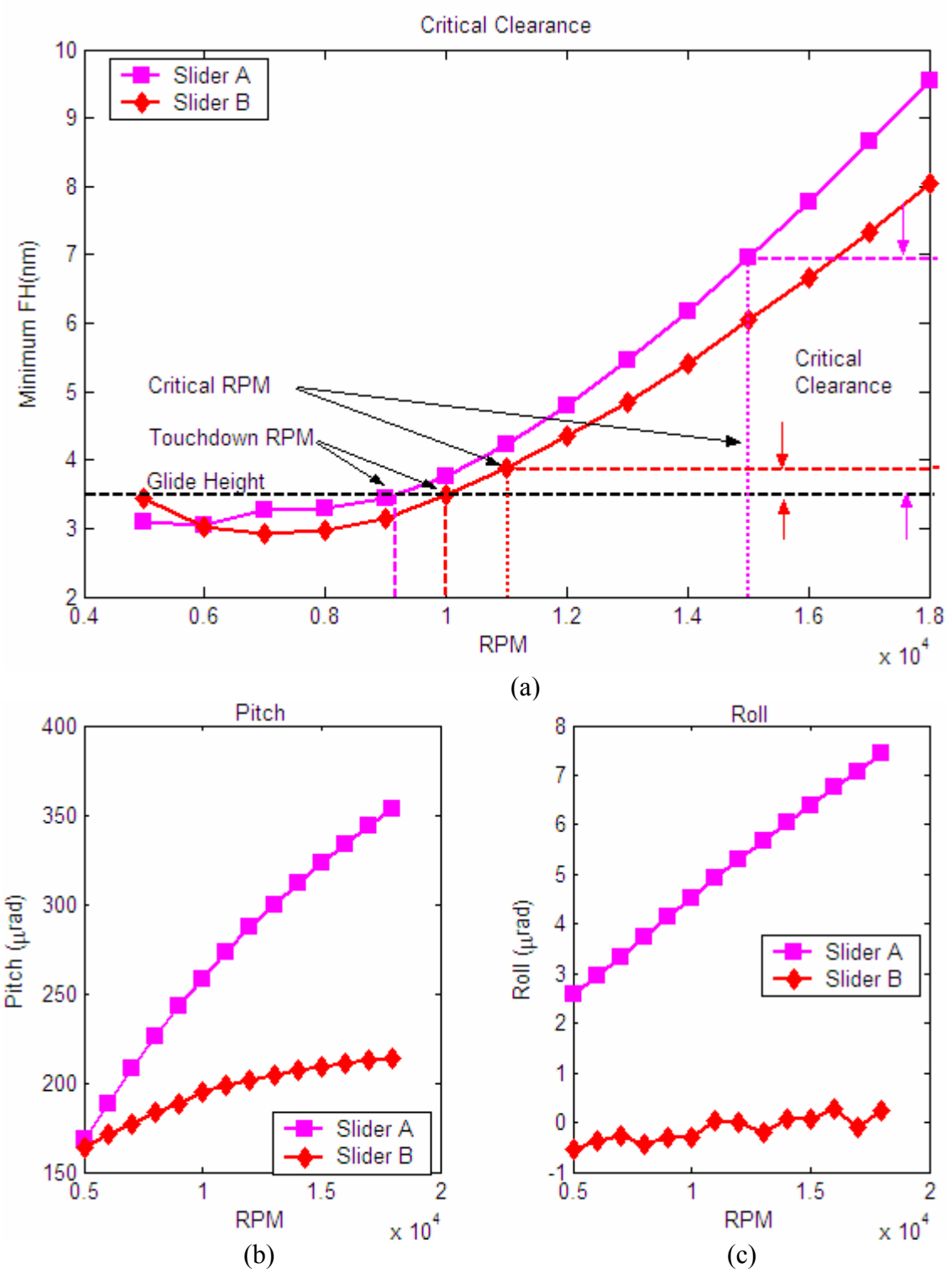


**Figure 21: (a): Critical clearance and Minimum fly height for Femto A and B; (b), (c): Pitch and Roll of Femto A and B, respectively**

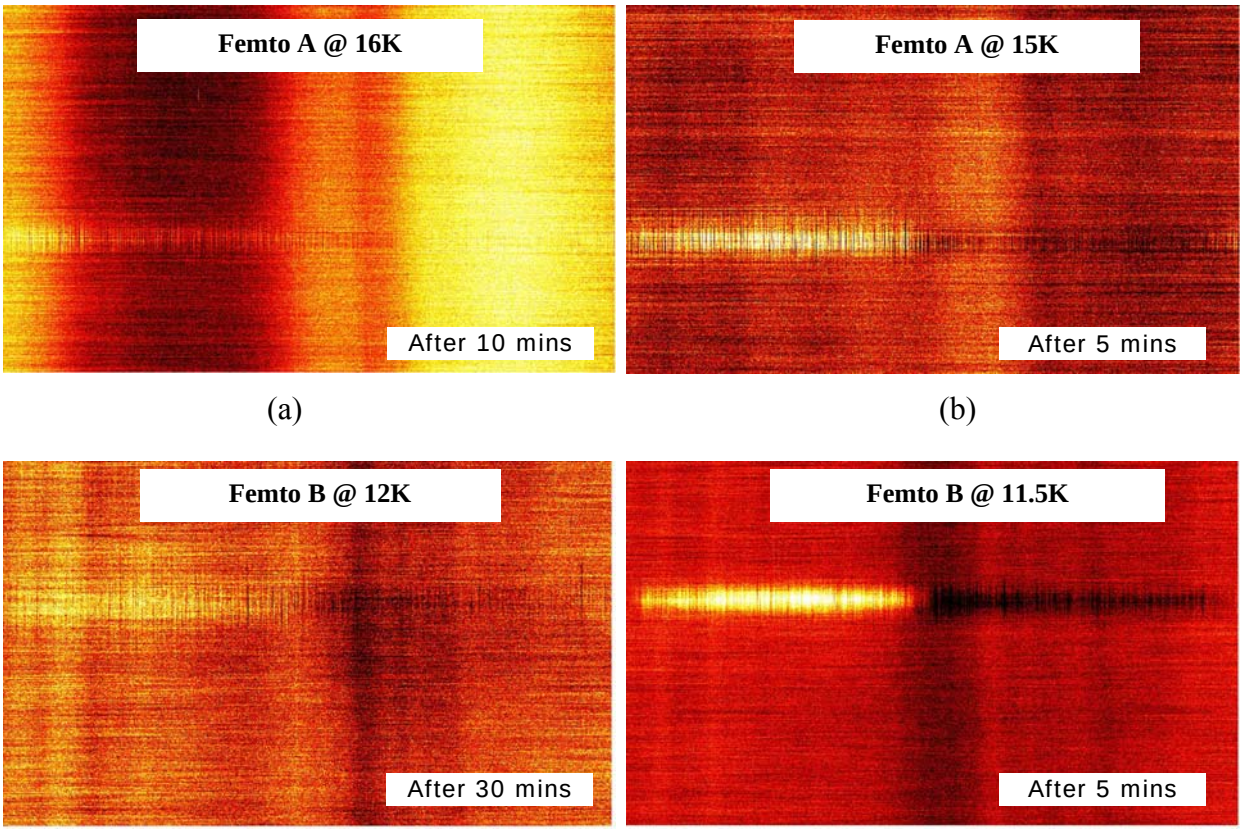


**Figure 22: (a) ,(c): Femto A and B above critical rpm showing less depletion and transfer, respectively; (b), (d): Femto A and B at critical rpm showing greater depletion and transfer, respectively**